Downloaded from https://www.lyellcollection.org by INIST-CNRS on Jun 16, 2026

Channelized sandstone bodies ('cordons') in the Tassili N'Ajjer (Algeria & Libya): snapshots of a Late Ordovician proglacial outwash plain

F. GIRARD[1]*, J.-F. GHIENNE[1] & J.-L. RUBINO[2]

[1]*Ecole et Observatoire des Sciences de la Terre, Institut de Physique du Globe de Strasbourg, UMR 7516 CNRS – Université de Strasbourg, 1 rue Blessig, 67084 Strasbourg, France*

[2]*Total S.A., CSTJF, Avenue Larribau 64018 Pau Cedex, France*

**Corresponding author (e-mail: fgirard@unistra.fr)*

Abstract: The architecture, distribution and development of channelized sandstone bodies are described from Late Ordovician paraglacial successions of the Tassili N'Ajjer (SE Algeria and SW Libya) based on satellite images and field data (sedimentary logs, photomosaics). Sandstone bodies have a ribbon-like form at outcrop (often referred to as 'cordons' in the literature). They typify a fluvioglacial outwash plain deposited between a continental ice front and a marine delta-front zone. Channelized sandstone bodies are straight to sinuous, with widths (W) in the 60–600 m range, thicknesses (T) in the 5–30 m range and they have a mean W/T ratio of 16.5. They develop within an aggradational–progradational sand-dominated deltaic topset succession including at its distal end a terminal distributary channel and mouth-bar environments. The architecture of channel bodies and the related depositional facies, which includes climbing-dune cross-stratification, indicates that channelized sandstone bodies represent plugs of isolated channels related to high-magnitude flood events (glacier outbursts). These plugs form fossilized networks of both braided channels and interlaced anastomosed channels, offering snapshots of an outburst-related unconfined proglacial outwash braidplain constituted by the amalgamation of adjacent, elongated outwash fans.

The Late Ordovician (Hirnantian) glaciation was responsible for deposition of a thick sand-dominated wedge (Eschard *et al.* 2005; Le Heron *et al.* 2006; Ghienne *et al.* 2007*a*), and correlative sandstones in the subsurface frequently constitute valuable hydrocarbon reservoirs that contain large volumes of recoverable hydrocarbon reserves, especially in North Africa and Arabia (e.g. Hirst *et al.* 2002; Le Heron *et al.* 2006, 2009; Galeazzi *et al.* 2010). The present contribution provides a detailed analysis of fluvioglacial channel networks in southwestern Libya and southeastern Algeria. Related heterogenities may have in part controlled fluid flows through the glaciogenic reservoirs. Documenting pro-glacial outwash plain deposits is therefore important to understand the architecture and facies model of glaciogenic petroleum reservoirs.

The ability to identify former fluvial systems based on their stratigraphical record, from their internal organization (Miall 1996) and/or from the geometry of resulting sediment bodies (Friend 1983; Gibling 2006) is not straightforward. Despite the considerable amount of research that has been conducted on modern (Boothroyd & Nummedal 1978; Maizel 1993, 1997; Gomez *et al.* 2000; Magilligan *et al.* 2002; Carrivick & Russell 2007; Duller *et al.* 2008) and Pleistocene (Church 1972; Dawson & Bryant 1987; Krzyszkowski 2002; Zielinski & Van Loon 2002, 2003; Winsemann *et al.* 2009) sandur-type plains, and although channel networks on pro-glacial outwash plains are used as prototypes of braided river systems (e.g. Zielinski & Van Loon 2002, 2003; Marren 2004 and references therein), fluvial channel bodies of pro-glacial outwash plains have received much less attention than those of braided or meandering end-member rivers (Gibling 2006). In particular, relatively few accounts have dealt with channel responses to extreme fluctuations in runoff and sediment inputs upon the distal pro-glacial drainage system (e.g. Björnsson 2002; Snorrason *et al.* 2002; Marren 2005; Russell *et al.* 2005; Peters *et al.* 2007; Russell 2009).

Based on cross-sections and satellite images, this contribution successively explores sedimentary facies and the external geometry of channelized sandstone bodies – often referred to as 'cordons' in the literature – which are usually exposed in three dimensions, providing an outstanding record

From: Huuse, M., Redfern, J., Le Heron, D. P., Dixon, R. J., Moscariello, A. & Craig, J. (eds) 2012. *Glaciogenic Reservoirs and Hydrocarbon Systems*. Geological Society, London, Special Publications, **368**, 355–379.
First published online March 8, 2012, http://dx.doi.org/10.1144/SP368.3 © The Geological Society of London 2012.
Publishing disclaimer: www.geolsoc.org.uk/pub_ethics

Downloaded from https://www.lyellcollection.org by INIST-CNRS on Jun 16, 2026

of ancient pro-glacial outwash drainage networks. Considering that high-magnitude flood events have recently been inferred based on the occurrence of unusual sedimentary structures in the related depositional successions (Ghienne *et al.* 2010), the role of outburst-related processes on the fluvio-glacial architecture is then discussed. Finally, relationships with other non-glacial potential analogues are outlined.

Context

Geological setting

The Tassili N'Ajjer plateau comprises Cambrian to Ordovician sandstone strata deposited upon the Hoggar Shield at the southern edge of the Illizi Basin (SE Algeria) and at the western edge of the Murzuq Basin (SW Libya) (Fig. 1a). Throughout

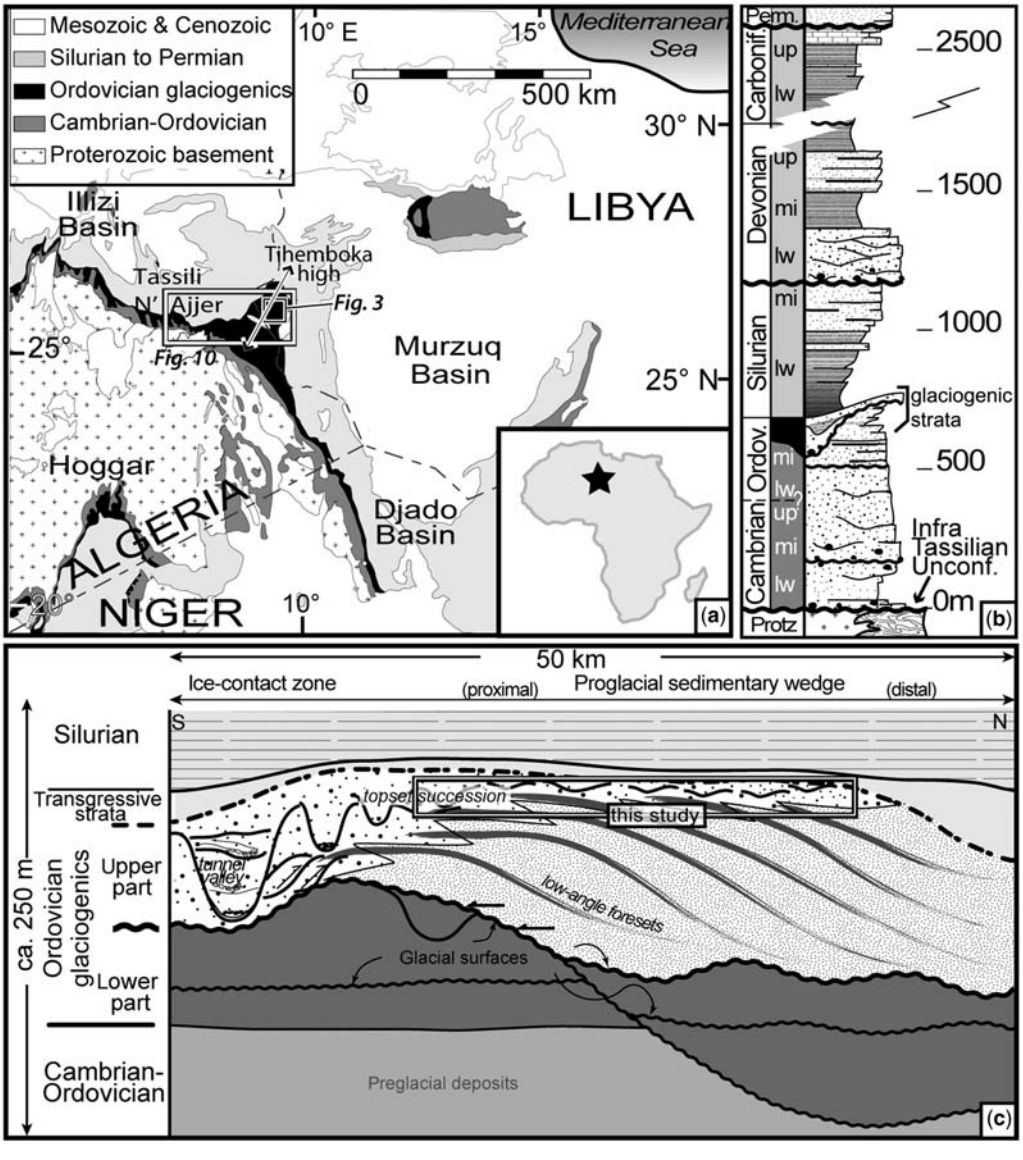

Fig. 1. (**a**) Geological sketch map with location of the study area in western Libya (western Murzuq Basin) and eastern Algeria (Tassili N'Ajjer Plateau). The Tihemboka structural high separates the Murzuq and Illizi basins. (**b**) Synthetic Palaeozoic succession in the Murzuq Basin. (**c**) Stratigraphic framework of the sedimentary wedge.

Downloaded from https://www.lyellcollection.org by INIST-CNRS on Jun 16, 2026

its Palaeozoic to Cenozoic evolution, the corresponding area was a stable intra-plate domain, with tectonic uplifts individualizing several intracratonic basins, the present geometry of which bears little relation to the broader North Gondwana platform that had an off-shelf gradient toward the NNW throughout the early Palaeozoic (Beuf *et al.* 1971; Coward & Ries 2003; Fabre & Kazi-Tani 2005; Galeazzi *et al.* 2010). Structural highs, such as the Tihemboka High, trend SSW–NNE, separating the Illizi and Murzuq basins, and were recurrently active during the Palaeozoic. At the first order, the Lower Palaeozoic succession consists of a Cambrian to Ordovician transgressive sedimentary package (fluvial to shallow-marine succession), an uppermost Ordovician, erosively based, glacially related unit, and a Silurian to Lower Devonian regressive package (inner shelf to fluvial) (Bellini & Massa 1980; Eschard *et al.* 2005; Ghienne *et al.* 2007*b*) (Fig. 1b).

In the latest Ordovician (Hirnantian stage, <2 Ma in duration), a continental-scale ice sheet extended from present-day West and North Africa, to Arabia, possibly joining South Africa (Ghienne *et al.* 2007*b*). In places, high-frequency ice-front advance and retreat cycles resulted in up to five erosively based, vertically superimposed and laterally juxtaposed, glacial depositional sequences. They essentially comprise pro-glacial to interglacial successions with a range of fluvial, deltaic and shallow-marine deposits passing distally into turbiditic deposits (Ghienne 2003; Le Heron *et al.* 2006; Ghienne *et al.* 2007*a*). Each of the depositional sequences fills in palaeovalleys, glacial troughs or depressions, some of which represent former ice-stream pathways (Moreau *et al.* 2005; Ghienne *et al.* 2007*b*; Le Heron & Craig 2008). Together, glacial striations and mega-scale lineations, tunnel valleys and fluvioglacial palaeocurrents document a relatively uniform pattern of palaeoflows at the scale of the glaciated platform.

Depositional setting

The channels described in this contribution represent a late stage of a glacial evolution subsequent to the Hirnantian glacial maximum (Ghienne *et al.* 2007*a*; Loi *et al.* 2010). They are included in the upper part of a 50–150 m thick glacially related depositional sequence, which onlaps the last basin-wide glacial erosion surface characterized by subglacial palaeolandforms (Figs 1c & 2). A latest and subordinate glacial surface and overlying post-glacial transgressive strata (Fig. 1c) truncate the sequence. To the south, ice-front, subglacial and ice-marginal environments are inferred from the occurrence of a glaciotectonic fold-and-thrust belt and tunnel channels indicating a connection between a subglacial drainage network and the studied channels (Figs 1c & 2). Northward of this ice-proximal zone, and in stratigraphic connection with it, a sand-dominated, coarsening-upward sedimentary wedge is preserved. It displays a marine deltaic topset/foreset/bottomset architecture (Figs 1c & 2). Delta plain topsets are essentially made up of medium- to coarse-grained sandstones. They include the studied fluvioglacial channels evidenced by kilometre-scale sandstone ribbons corresponding to inverted topographies (‘cordons’ of Beuf *et al.* 1971 and Hirst *et al.* 2002; see below the upper unit description, Fig. 3). This topset succession also comprises subaqueous terminal distributary

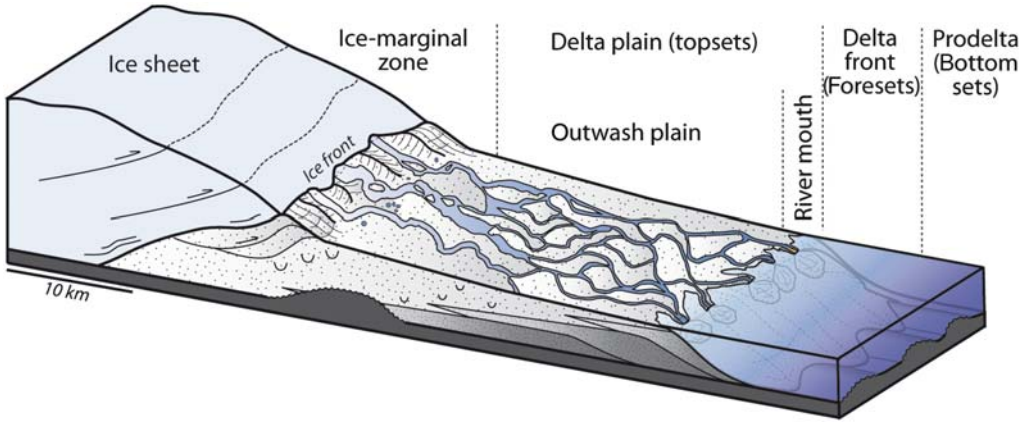

Fig. 2. Depositional setting of the channelized sandstone bodies. Channel networks develop in a topset succession between an ice-marginal zone to the south and river mouths to the north. The related sediment wedge onlaps a glacial surface including palaeotopographies.

Downloaded from https://www.lyellcollection.org by INIST-CNRS on Jun 16, 2026

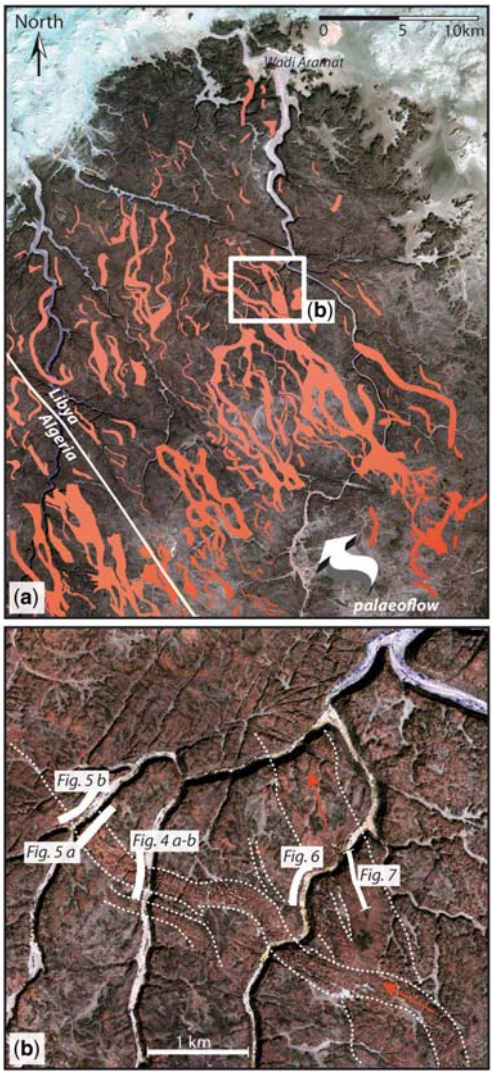

Fig. 3. (**a**) Mapping of channelized sandstone bodies forming sandstone ribbons ('cordons') in SW Libya, Tihemboka area (Spot image, palaeoflow towards the NNW). (**b**) Detailed view in the Wadi Aramat area with location of studied outcrops and photomosaics.

channels (transitional unit) and mouth-bar deposits showing, in places, bioturbation (*Arenicolites*, see lower unit description). In the southern proximal region, the fluvioglacial topset succession is up to 60 m thick. It progressively thins and eventually pinches out downstream to the North at the 50 km scale (Figs 1c & 2). Climbing-dune cross-stratification (CDCS), interpreted as the result of glacial outburst events, characterizes the fluvioglacial channels of the topset succession and their transition with upper foresets (Ghienne *et al.* 2010). Foresets are characterized by medium- to coarse-grained erosively based sandstone sheets, 2–12 m in thickness, which alternate with relatively thick (5–25 m) fine-grained intervals comprising silty shales to muddy fine-grained sandstones. Foresets have maximum dip angles of 5–10 m km^{-1} (i.e. $<1^{\circ}$), and are typically 40–60 m in height. Bottomset deposits are made up of 2–10 m thick medium-grained rippled or structureless sandstone beds, alternating with thinner (0–10 m) argillaceous fine-grained intervals. Upper horizons of the fluvioglacial topset succession are in places intensively deformed, with folds and thrusts affecting an up to 15 m thick sandstone pile, indicating a late glaciotectonic deformation. Truncating the upper part of the fluvioglacial topset succession, erosional transgressive surfaces (wave, tide) and associated bioturbated sandstones bearing macrofaunas highlight the post-glacial transgressive strata (Fig. 1c).

The sedimentary wedge that includes the fluvioglacial channels is interpreted to reflect fluviodeltaic progradation, which includes outwash plain/delta-plain topsets (the subject of the present study), delta-front foresets and lobe-related bottomsets (Ghienne *et al.* 2010) (Figs 1c & 2). The thick (40–60 m) delta-plain topset succession to the south, pinching out to the north, allows a slope gradient of the palaeo-depositional surface to be estimated in the 0.5–2 m km^{-1} range. The shallow-marine coastal setting of the fluvioglacial delta is indicated by the *Arenicolites*-type bioturbation. The lack of any ice-rafted debris in foreset and bottomset argillaceous fallout suspension deposits indicates that no glaciomarine ice front occurred at the time of delta development, at least within the study area. The topset succession, including the studied channel bodies, then belonged to an aggrading sandur-type pro-glacial fluvio-deltaic setting and was deposited between a continental ice front to the south and a sea to the north. Ice-marginal fluvioglacial depositional environments, aggradational fluvioglacial deltaic topsets and related downcurrent delta development most probably relate to a period of ice-front advance (e.g. Maizels 1997; Marren 2002, 2005; Russell *et al.* 2005; Smith *et al.* 2006). As the succession onlaps the last basin-wide glacial surface and is overlain by the post-glacial shallow-marine transgressive strata, deposition is thought either to have occurred during an ice-front stillstand or short-lived re-advance (glacial surge?) within an overall ice-sheet recession period, or to be associated with the ultimate advance of the Hirnantian ice sheet across the study area.

Methods

Channel bodies have been studied at the outcrop scale based on detailed sections and profiles in a

Downloaded from https://www.lyellcollection.org by INIST-CNRS on Jun 16, 2026

restricted area (4 × 5 km) in SW Libya (Fig. 3) (Wadi Aramat, Tihemboka area), and at a regional scale based on their spatial distribution as seen on satellite images extending from SE Algeria to SW Libya (Tassili N'Ajjer, 250 × 100 km). Internal architecture and facies successions in sandstone bodies were investigated along walls of wadi canyons up to 50 m in height cutting Late Ordovician channel bodies transverse to palaeoflow orientations (Figs 3–7). Measured cross-sections were logged at a scale of 1:100, noting grain size, bed thickness, bed contacts and geometry, sedimentary structures and palaeocurrent directions. Eight depositional facies (F1 to F8, numbers increasing with grain size) have been described and interpreted (Table 1 & Fig. 8). High-resolution Spot, Alos and Google Earth™ satellite images were used to unravel external geometries and trends in orientation, and to map the distribution of about 300 channel bodies. In the case of channel bodies that crop out as inverted topographies, channel-body thicknesses were derived from the SRTM30 Digital Elevation Model included in the Google Earth™ software.

Outcrop-scale channel architecture

In the Wadi Aramat area, natural sections of large-scale channel bodies are provided by canyon incisions with kilometre spacing (Figs 3–7). Small-scale individual channel bodies (Fig. 6) are also connected to the larger ones. Channel bodies are amalgamated with underlying more sheet-like sandstone bodies. Their superimposition results in 25–40 m thick compound sandstone bodies that are made of three vertically superimposed units (from base to top: lower, transitional and upper units) constituting the fluvioglacial deltaic topset succession. Although only the upper unit includes channelized sandstone bodies that are ascribed to fluvial depositional environments, the entire topset succession is described and interpreted in order to show the stratigraphic architecture of a prograding mouth-bar/fluvial channel system in the topsets of the proglacial fluviodeltaic wedge.

Lower unit description

The lower unit includes very thick sandstone beds (yellow colour in Figs 4–7) alternating with successions of thinner sandstone beds (green colour in Figs 4–7). The former are 4–10 m thick, several kilometres wide, tabular, medium-grained sandstone bodies, with flat, erosional bases showing rare flute casts and common large-scale load and flame structures. They extend basinward into the foreset succession and correspond to the erosion-based sandstone sheets of Ghienne *et al.* (2010). Thick sandstone beds are entirely laminated, including mainly crudely defined ripple lamination (F4) or horizontal to subhorizontal laminations (F3) grading upwards into two-dimensional CDCS (F5; Ghienne *et al.* 2010). Vertical sheet-dewatering structures are commonly present at bed tops.

Intervening successions (green colour in Figs 4–7) include sharp-based, thin (0.3–1.5 m thick), medium-grained sandstone beds and some relatively rare <0.5 m finer-grained interbeds. Lower bed contacts display decimetre-scale gutter casts and common load casts. Horizontally to subhorizontally laminated medium-grained sandstone (F3) predominates. Bed tops are associated with either ripple trains locally developing into stoss-depositional climbing ripples assemblages (F2) or lags of small (<5 cm) rip-up clasts. Sandstone beds are generally stacked, but interbeds of very fine-grained sandstones to siltstones (F1) are present in places, indicating occasional fining-upward trends at a bed/interbed scale. Vertical sheet-dewatering structures are ubiquitous (Fig. 8f). In places, tracks and vertical U-shape burrows can be found, some of which are of the type *Arenicolites* (Fig. 8a).

Transitional unit description

The transitional unit is typically made up of several-metre-thick, tabular, erosion-based medium-grained sandstone bodies (orange colour in Figs 4–7). Vertical stacking forms a distinctive set of two to four, but more generally three, amalgamated bodies (Fig. 7). They together constitute a 5–15 m thick sandstone sheet that has a lateral extent of several kilometres (Figs 4–6). The latter interdigitates laterally with thinner-bedded successions comparable to those of the intervening succession of the lower unit (green colour in Fig. 6). Regarding the lowest tabular sandstone body, a basal, poorly differentiated shallow scour may exist, with 1–5 m incision depths and up to 100 m in width. The scour is preferentially positioned in the axis of overlying channelized sandstone bodies of the upper unit (Fig. 4a, b) and is generally associated with metre to several metre-wide gutter casts, uncommon flute casts and lags of 1–10 cm long rip-up clasts and/or intraformational conglomerate lenses (F8) (Fig. 8d). At the lower bounding surface of the transitional unit, scouring results locally in the amalgamation of the tabular sandstone bodies with the underlying erosion-based sandstone sheets of the lower unit. At its upper bounding surface, and approaching the axis of an overlying channelized sandstone body, thick tabular bodies of the transitional unit locally thicken, resulting in convex-up geometries and clinoform-like structures in views transverse to palaeoflows (Fig. 4a, b).

Downloaded from https://www.lyellcollection.org by NIST-CNRS on Jun 16, 2026

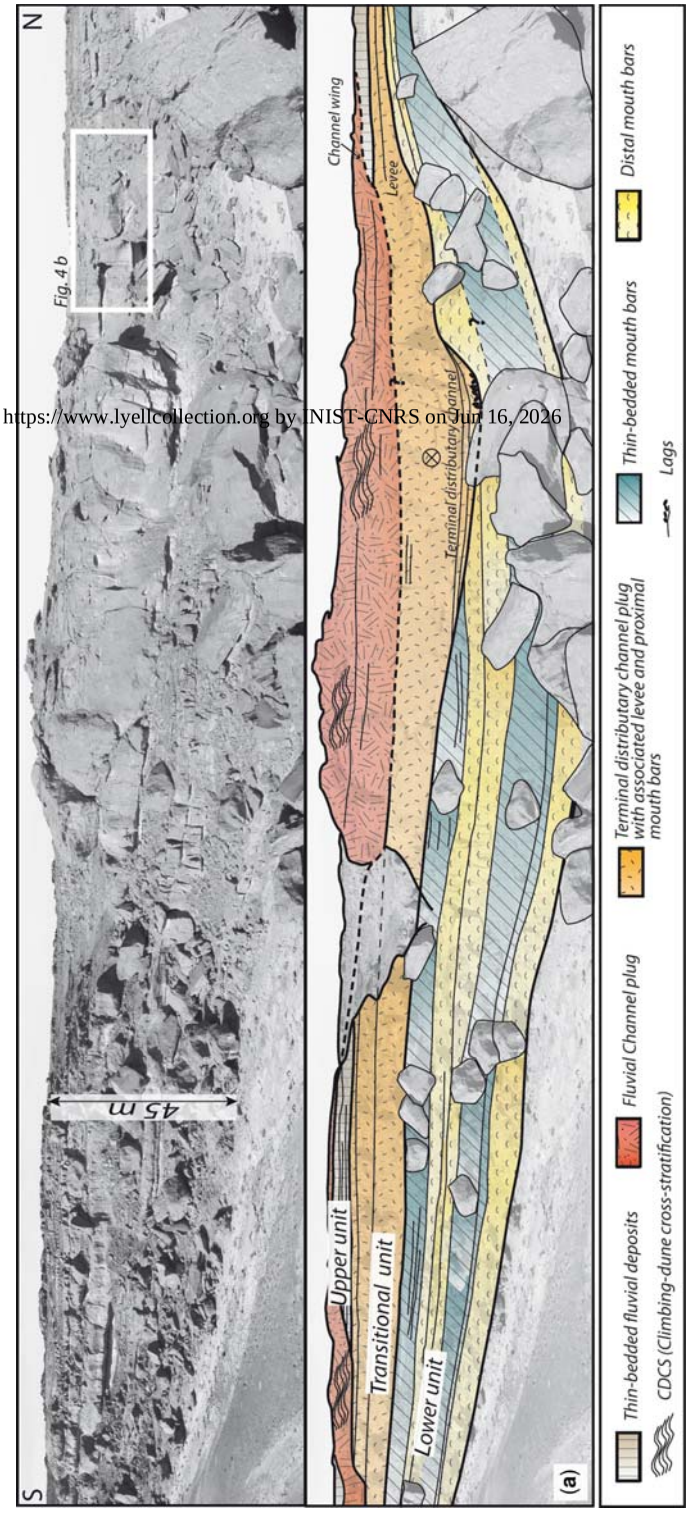

Fig. 4. Photomosaics showing relationships between architectures (line drawings) and related depositional environments (colour ranges) in the lower, transitional and upper units (see Fig. 3 for location). (**b**) Detail of (**a**), showing the levee architecture associated with the transitional unit.

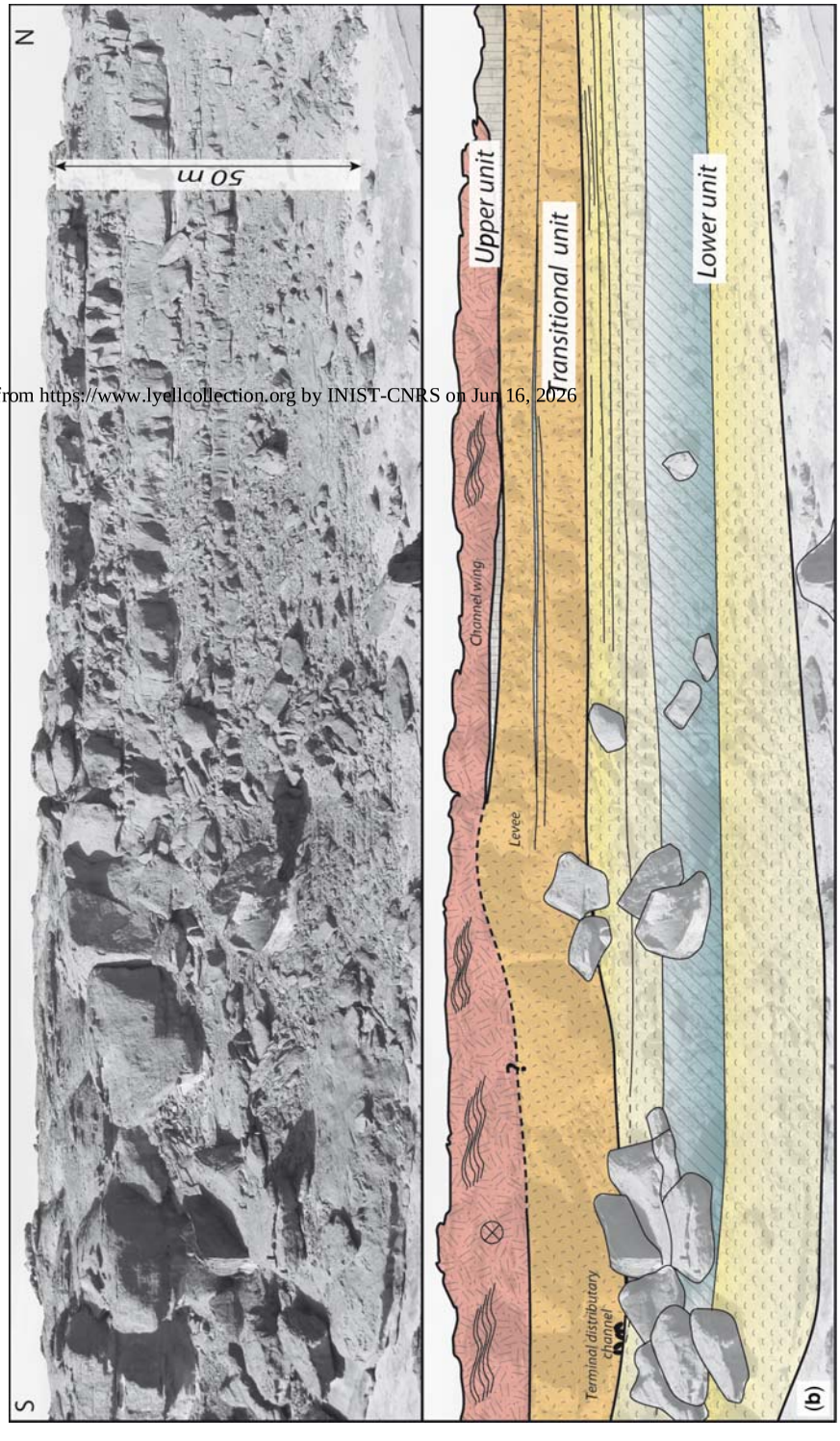

Downloaded from https://www.lyellcollection.org by INIST-CNRS on Jun 16, 2026

Fig. 4. *Continued.*

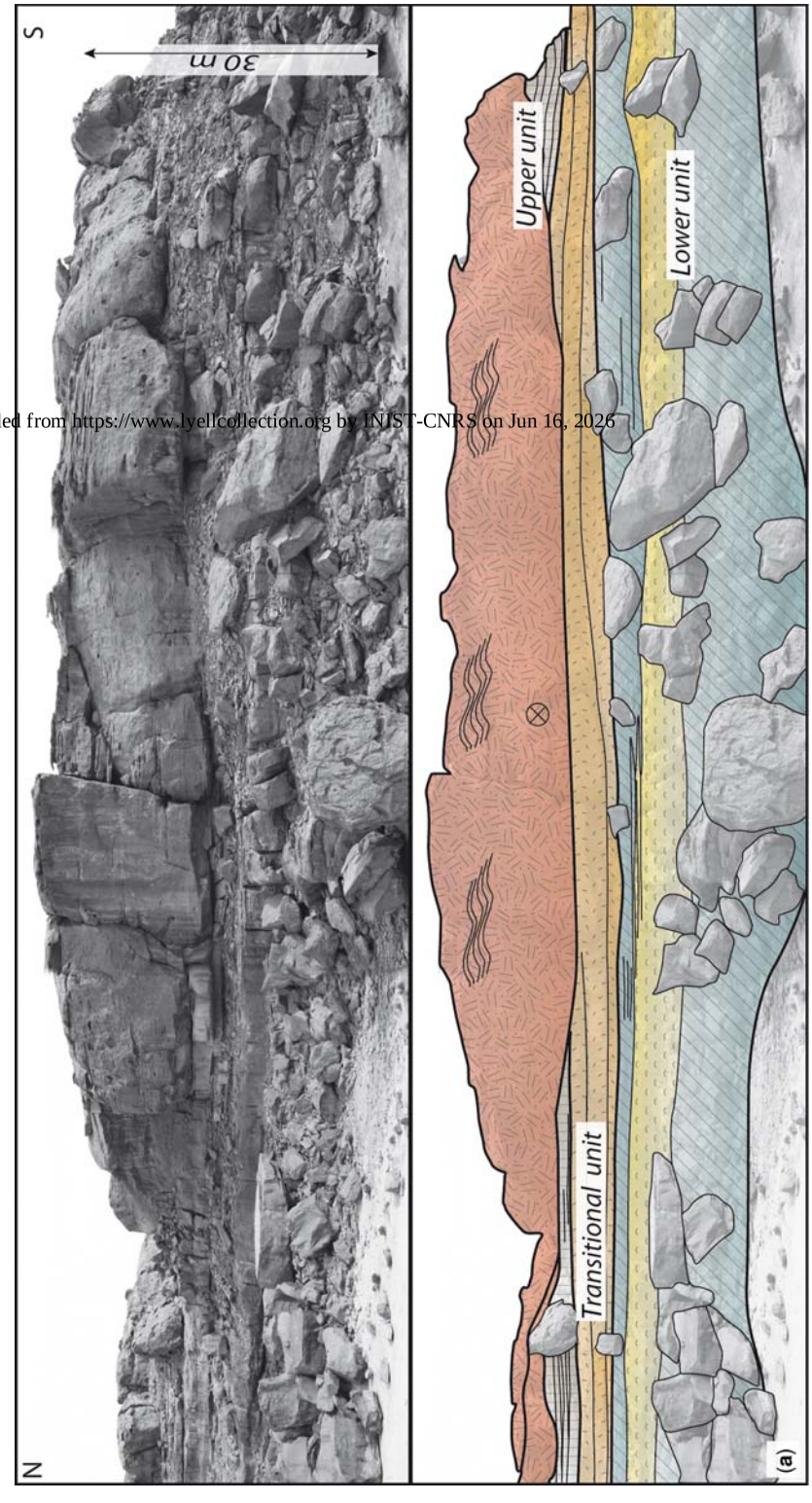

Downloaded from https://www.lyellcollection.org by INIST-CNRS on Jun 16, 2026

Fig. 5. Photomosaics showing relationships between architectures (line drawings) and related depositional environments (colour ranges) in the lower, transitional and upper units within the same compound sandstone bodies as in Figure 4, but 1 km further downstream. (**a**) and (**b**) illustrate the same structure seen on opposite sides of the wadi (see Fig. 3 for outcrop location sections and Fig. 4a for colour ranges).

Downloaded from https://www.lyellcollection.org by INIST-CNRS on Jun 16, 2026

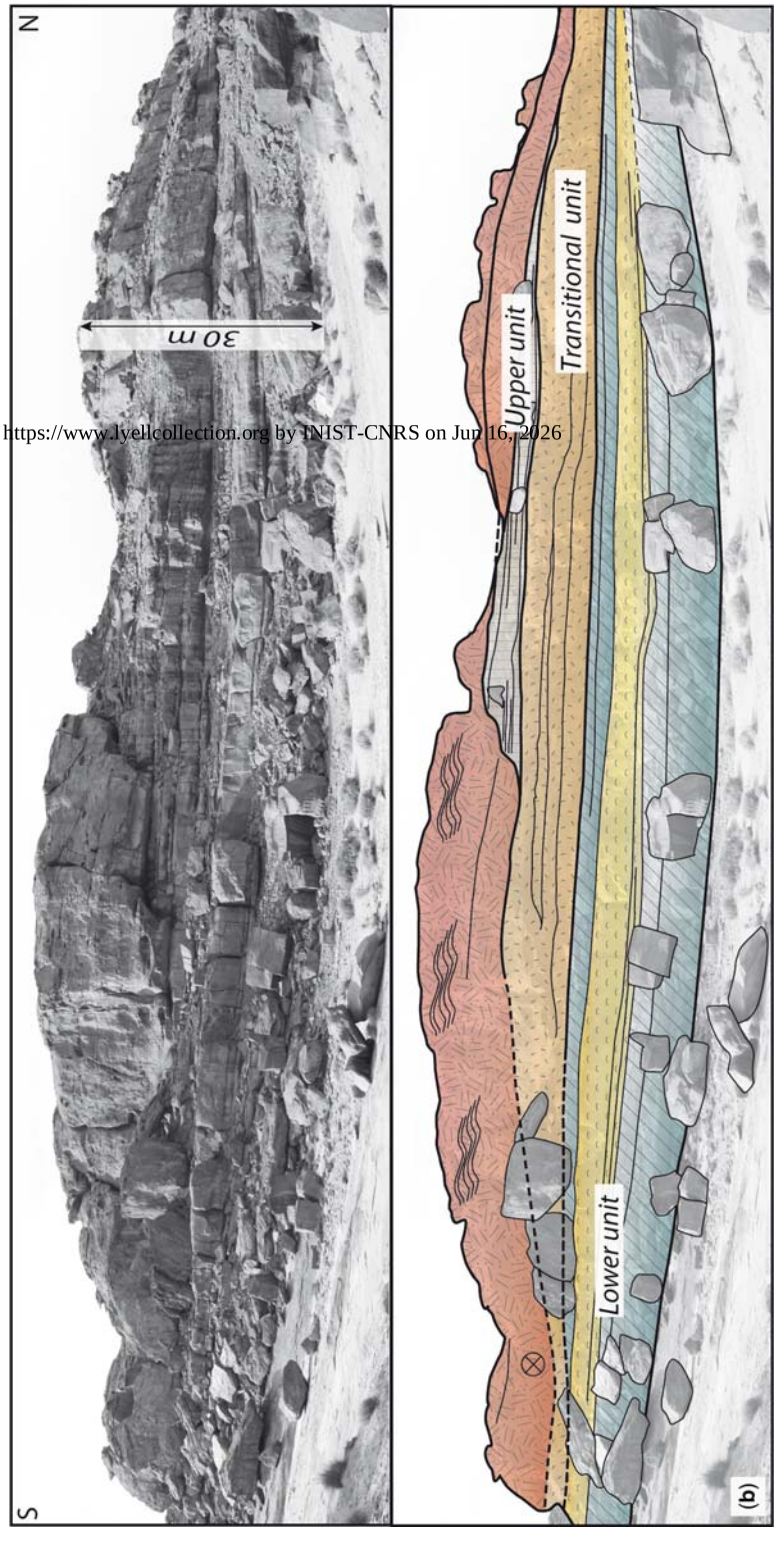

Fig. 5. *Continued.*

Downloaded from https://www.lyellcollection.org by INIST-CNRS on Jun 16, 2026

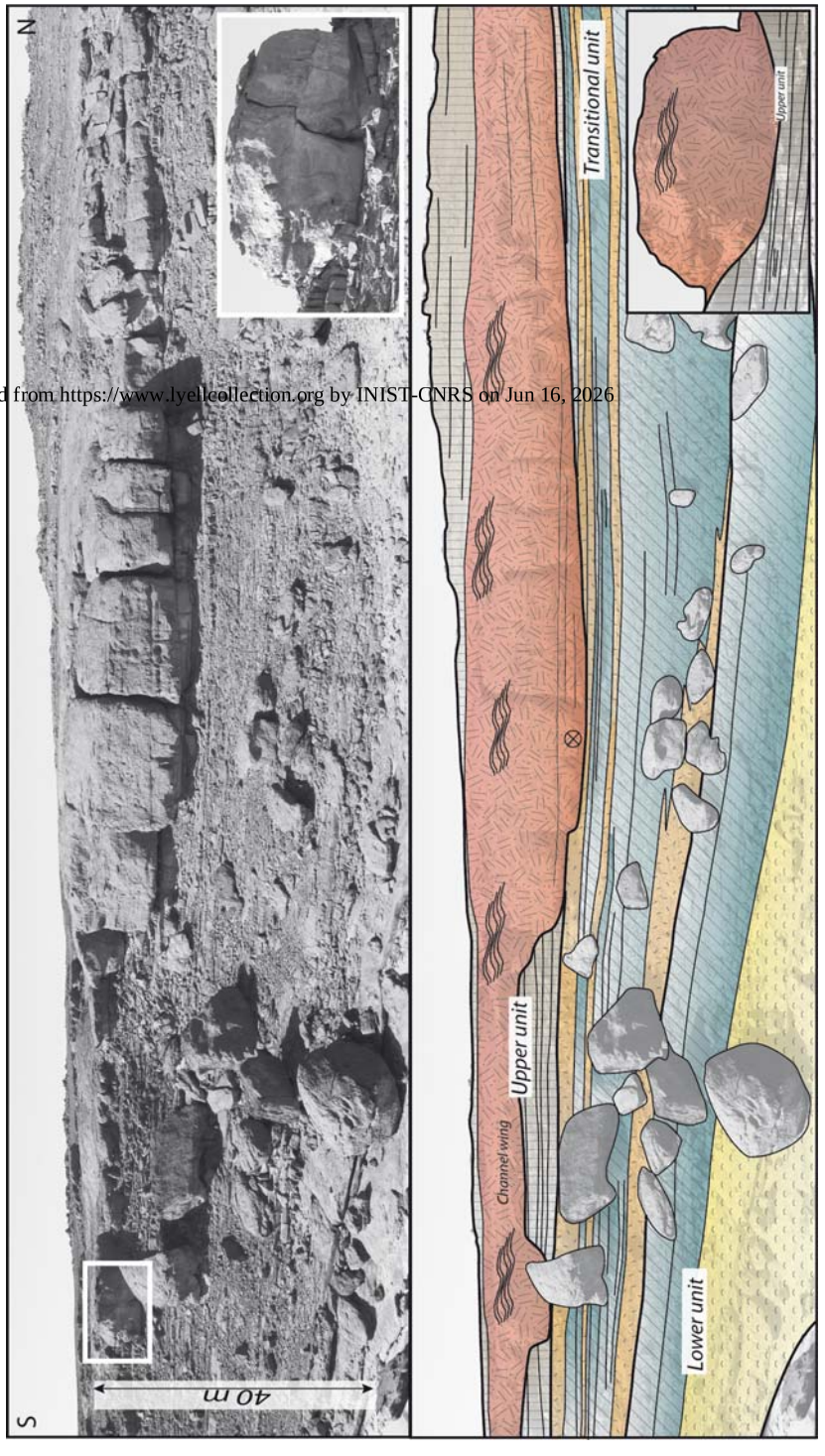

Fig. 6. Photomosaics showing relationships between architectures (line drawings) and related depositional environments (colour ranges) in the lower, transitional and upper units within another compound sandstone body (see Fig. 3 for outcrop location sections and Fig. 4a for colour ranges). Inset: detail of an adjacent small-scale channelized sandstone body.

Downloaded from https://www.lyellcollection.org by INIST-CNRS on Jun 16, 2026

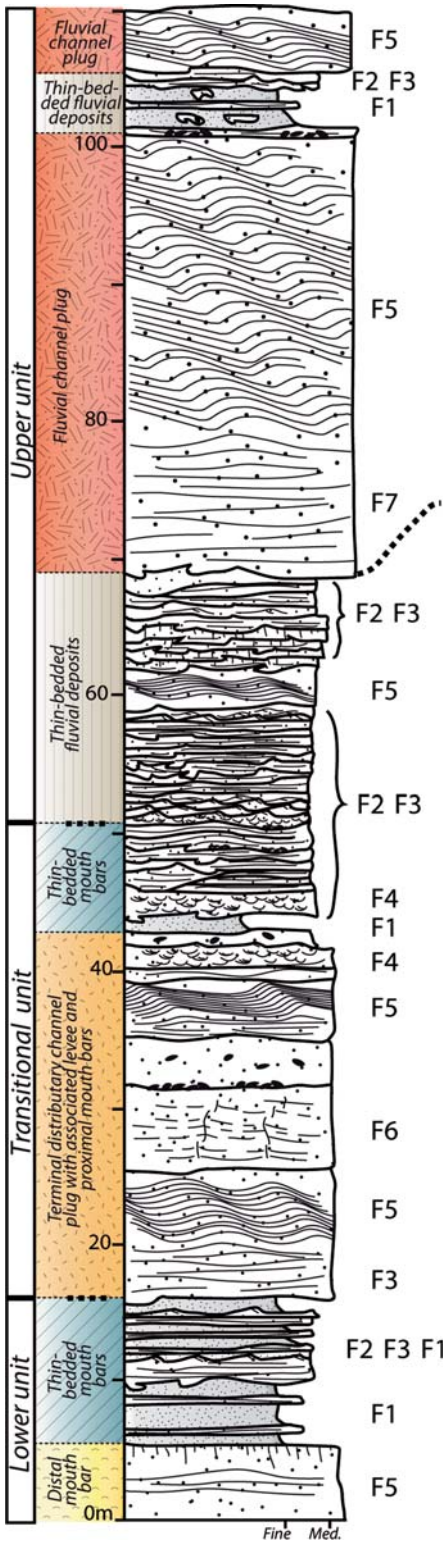

Fig. 7. Sedimentary log illustrating the depositional pattern in the lower, transitional and upper units (see Fig. 3 for location and Fig. 4a for colour ranges). Facies codes are given in Table 1.

Facies associations are similar to those of the lower unit, especially regarding thin-bedded successions, with identical depositional facies and *Arenicolites*-type bioturbation in places. Thick tabular sandstone bodies of the transitional unit may, however, differ, with less represented two-dimensional CDCS (F5) and the occurrence of a distinct climbing cross-stratification that involve undulating, low-relief almost symmetric bedforms (F6, Fig. 8e). Away from shallow scours, amalgamation of the thick sandstone bodies may decrease, with intervening stoss-depositional climbing ripple assemblages (F2) and rare fine-grained intervals (F1) preserved in interbeds. Both thick and thin sandstone beds show vertical sheet-dewatering structures.

Upper unit description

The upper unit comprises channelized bodies corresponding to sandstone ribbons at outcrop, either large-scale (Figs 4–6) or small-scale features (Fig. 6), and inter-channel thin-bedded deposits. Its lower contact is conformable where thin-bedded deposits are present in the lower part of the unit, but erosional truncations with locally steep margins (up to 30°) may occur in the axis of some large-scale channel bodies. Large-scale channel bodies consist of packages of amalgamated sandstones, whereas inter-channel thin-bedded deposits correspond to well-stratified successions. The latter comprise tabular, 0.5–2 m thick, erosion-based sandstone beds including mainly horizontal lamination (F3) associated with ripple cross-stratification (F2; Fig. 8b). Lags of small (<5 cm) rip-up clasts on top of the beds are frequent (Fig. 7). In contrast with similar depositional facies from the underlying units, they are virtually devoid of any dewatering features.

A poor bedset differentiation characterizes sandstones of large-scale channel bodies. Deposits at the channel axis correspond to a fining-upward sandstone suite. At the base, it comprises several-metre-thick bedsets with large (>10 m) bedform wavelengths resulting in poorly defined undulating to low-angle laminations (F7) (Fig. 8g, i). In its upper part, 2D and 3D CDCS (F5) predominates (Fig. 8h). The width of the large-scale channel body is typically in the 100–300 m range. Contacts between inter-channel deposits and large-scale channel bodies are erosional. Channel-body wings, also characterized by CDCS deposition, overstep inter-channel deposits and may in places connect with small-scale, less than 30 m wide, laterally

Downloaded from http://pubs.geoscienceworld.org/jsedres/article-pdf/81/5/362/3...

Table 1. *Lithofacies classification*

Facies (units)	Lithology	Main sedimentary structures	Bed or bedset thickness	Interpretation
F1 (Lu, Tu, Uu)	Siltstone to fine-grained sandstone	No structure, or faintly laminated	5 cm–1 m	Prevailing suspension fall-out deposits, some bedload deposition from low-density underflows
F2 (Lu, Tu, Uu)	Fine-grained sandstone (well sorted)	Current-ripple lamination, stoss-depositional climbing-ripple cross-stratification, pebble lags, decimetre-scale load structures, 3D ripple bedforms on bed tops in Uu	10 cm–1 m	Traction deposition from decelerating and/or expanding turbulent flows, with significant suspension fall-out in case of aggrading bedforms, lower-flow regime conditions
F3 (Lu, Tu, Uu)	Fine to medium-grained sandstone (moderately sorted)	Horizontal lamination with partling lineations (Fig. 8b); occasionally, small-scale subhorizontal to concave-up laminations in the lower part of sandstone beds (Fig. 8j); load structures; rare *Arenicolites*-type bioturbation in Tu (Fig. 8a) and sheet dewatering structures in Lu and Tu (Fig. 8f)	5 cm–2 m	Traction deposition from quasi-steady turbulent flow in upper-flow regime conditions; occasional antidune deposits (Langford & Bracken 1987; Alexander *et al.* 2001), upper plane beds otherwise
F4 (Lu, Tu)	Medium-grained sandstone (poorly sorted)	Crude ripple cross-stratification (1–2 cm deep scours, faint lamination throughout, occasionally superimposed on larger scale bedforms, Fig. 8c), vertical sheet dewatering structures (sheets are 10–50 cm in height, 0.3–5 cm in width)	1–7 m	Reworking by low-energy currents of sand-dominated plume fall-out, re-deposition as tractive bedload layers (quasi-steady lower-flow regime condition without sustained bedload transport); high rate of deposition; water escape processes
F5 (Lu, Tu, Uu)	Medium-grained sandstone (moderately sorted)	Two-, occasionally three-dimensional (Uu) climbing-dunes cross-stratification, stoss-depositional to vertically aggrading (CDCS, wavelength <5 m, Fig. 8h)	1–10 m	Turbulent deposition from sustained decelerating and/or expanding turbulent flows, with high sand-sized suspension-load concentration (Ghienne *et al.* 2010), lower-flow regime conditions
F6 (Tu)	Medium-grained sandstone (moderately sorted)	Vertically aggrading, low relief, symmetrical and undulating lamination, episodic crestal jumps (wavelenght <1 m, Fig. 8e)	5 cm–1 m	Traction deposition from quasi-steady turbulent flows in upper-flow regime conditions (stationary antidunes in underflows, Spinewine *et al.* 2009)
F7 (Uu)	Medium- to coarse-grained sandstone (poorly sorted)	Horizontal to subhorizontal, thick (5–15 cm) laminations, representing large-scale undulating bedforms (up to 40 m in wavelength, 0.5–2 m in height, Fig. 8g,i)	1–10 m	Traction deposition from turbulent flows in upper-flow regime conditions and high sand-sized suspension load, at the transition from upper-plane beds to migrating and/or stationary antidunes (Fielding 2006; Duller *et al.* 2008).
F8 (Tu, Uu)	Intraformational conglomerates with a medium- to very coarse-grained sandstone matrix	Sandstone and siltstone clasts, massive or crude cross-stratification in places, decimetre- to metre-scale gutter casts and load structures (Fig. 8d)	1 cm–1 m	Bypass and cut-and-fill processes by turbulent flows, with prevailing upper-flow regime conditions

Lu, Tu, Uu: lower, transitional and upper units.

Downloaded from https://www.lyellcollection.org by INIST-CNRS on Jun 16, 2026

adjacent channel bodies. The basal scour of the latter, 2–10 m in depth, is either slightly concave-up or has more incised gutter-type geometries in association with intraformational conglomerates (F8). Both large-scale and small-scale channel bodies are sealed by well-stratified thin-bedded sandstone successions. As they include other subsequent channel bodies, they are similarly ascribed to inter-channel successions. Satellite images of the study area reveal that up to three generations of channel bodies with intervening inter-channel successions are locally superimposed (Fig. 3).

Compound sandstone bodies

Successive amalgamation of sheet-like sandstone bodies (lower and transitional units) and channelized sandstone bodies (upper unit) results in compound sandstone bodies that do not correspond to stratigraphic units, but favour the preservation of channelized sandstone bodies as inverted topographies (Fig. 3). Boundaries with laterally adjacent deposits are either erosional or diffuse (Fig. 5a, b). In the former case, they correspond to a true stratigraphic surface even if polyphased, while in the latter case, they look like erosional margins but are in fact of diagenetic origin or correspond to fractures. For instance, sandstone beds constituting the sheet-like transitional unit extend beyond apparent channel margins and amalgamate with sandstones constituting the sandstone bodies, and in particular those of the channelized sandstone body (Figs 4–7). If the ribbon geometry essentially reflects the plan-view shape of the channelized sandstone bodies of the upper unit, the compound sandstone body cross-section incorporates a thicker sediment pile partly cross-cutting stratigraphic architectures (Fig. 9).

Interpretation

In the context of a prograding deltaic wedge, compound sandstone bodies that result from the vertical stacking of sheet-like units with channelized bodies in their upper part are related to aggradational–progradational marine mouth-bar/channel systems (Figs 4–9). The above-described units reflect successive stages through time and space of the development of river mouths during delta advance. The *Arenicolites*-type burrows testifying shallow-marine environments are associated with the lower and the transitional unit, in good agreement with other occurrences of this bioturbation in restricted-marine environments such as mouth bars, tidal flats or bay-head deltas (Droser *et al.* 1994; Buatois *et al.* 2002; Gerard & Bromley 2008). We tentatively locate the subaerial/subaqueous boundary at the stratigraphic contact between the transitional essentially sheet-like unit and the upper unit that include channelized bodies. This position coincides with rare argillaceous interbeds upwards and with the disappearance of vertical sheet dewatering structures in the sedimentary record.

Geometries and facies in the lower unit indicate unconfined sand-dominated deposition from turbulent flows with both lower (F2, F4, F5) and upper (F3, F6) flow regime conditions. In particular, CDCS reflects a high concentration of sand-sized suspension load (Ghienne *et al.* 2010). At the scale of a thick sandstone bed, the basal erosion surface and the fining- and waning-upward trends are interpreted as reflecting expanding turbulent jets in front of terminal distributary channel mouths (Fig. 9b) (Sutter 1994; Edmonds & Slingerland 2007; Schomacker *et al.* 2010) and rapid sedimentation in distal mouth bar environments of a shallow water delta during the falling stage of a single short-duration, high-energy discharge event (Mellere *et al.* 2002; Mutti *et al.* 2003; Fielding *et al.* 2005). The downstream connection with the 'erosion-based sandstone sheet' case study of Ghienne *et al.* (2010), and occurrences of CDCS, demonstrate a flood dynamics involving highly concentrated sediment-laden flows. High depositional rates are in agreement with ubiquitous post-depositional water escape structures (Lowe 1975). Thinner beds in intervening successions reflect similar but minor flood events deposited under waning turbulent flows. They are interpreted as thin-bedded mouth bars (green colour in Figs 4–7 & 9).

The sheet-like architecture of the transitional unit reflects essentially unconfined sediment-laden flows even if confined flows were in places associated with basal scours. Basal erosion and intraformational conglomerates (F8) indicates bypass processes in a channelized area interpreted as a subaqueous terminal distributary channel (Plink-Björklund *et al.* 2001; Mellere *et al.* 2002; Olariu & Bhattacharya 2006) scoured by turbulent jet flow (Hoyal *et al.* 2003) (Figs 4 & 9) in front of a fluvial channel at the shore line. The clinoform-like geometries of sandstone bodies near the channel axis are interpreted as related to a subaqueous levee architecture that grades laterally and distally into proximal mouth bars (Figs 4 & 9) deposited as a result of the expanding jet flow in a lateral position relative to the axis of the scour (Fielding *et al.* 2005; Edmonds & Slingerland 2007; Schomacker *et al.* 2010). The whole depositional dynamic is fundamentally similar to that prevailing in the lower unit, but a more proximal location resulted in complete amalgamation of flood-related mouth-bar deposits in the form of vertically stacked, thick, tabular beds. Aggrading antidunes (F6) reflect shallower environments, but are still characterized by a high sand-sized suspension-load concentration

Downloaded from https://www.lyellcollection.org by INIST-CNRS on Jun 16, 2026

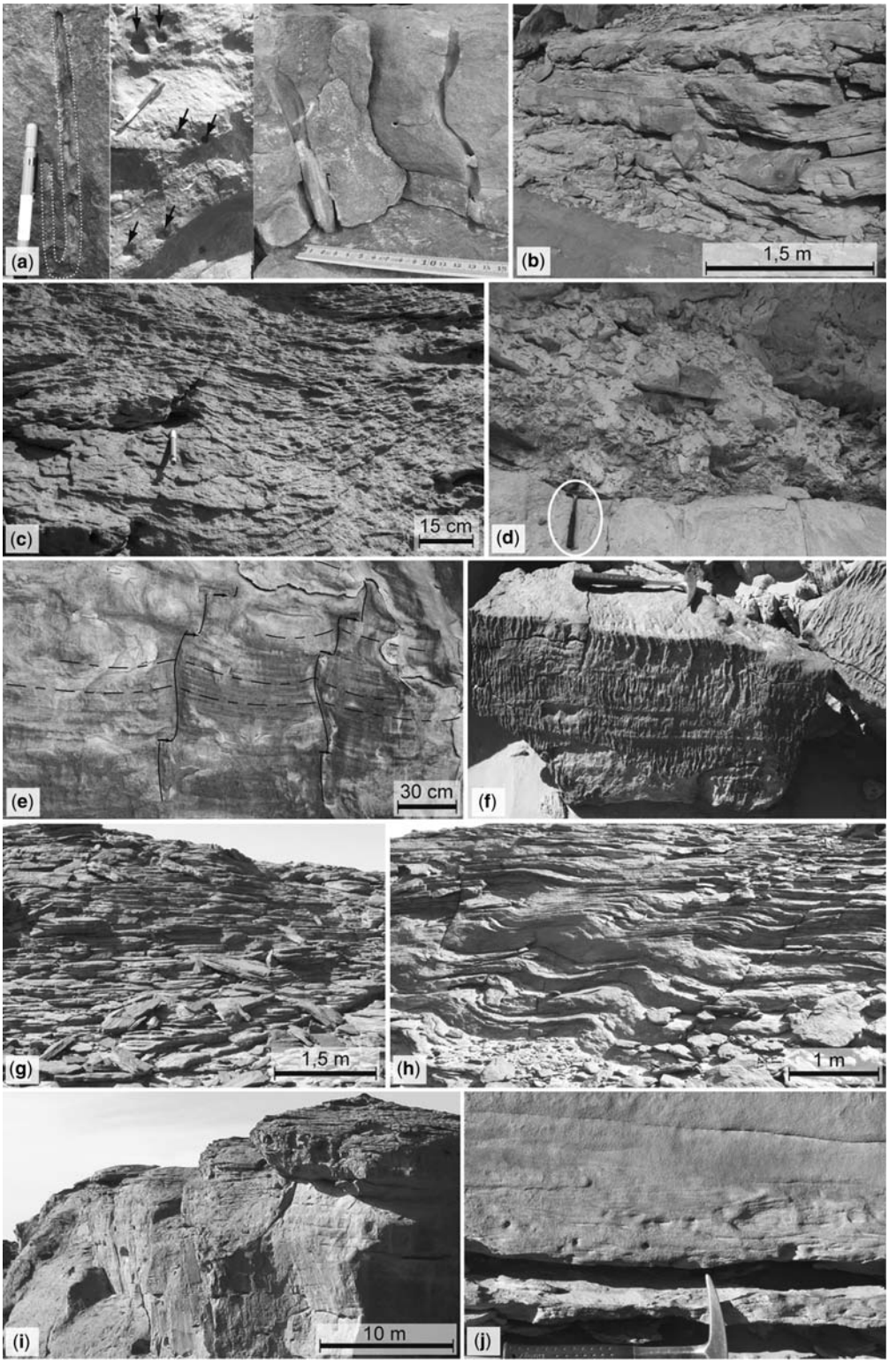

Downloaded from https://www.lyellcollection.org by INIST-CNRS on Jun 16, 2026

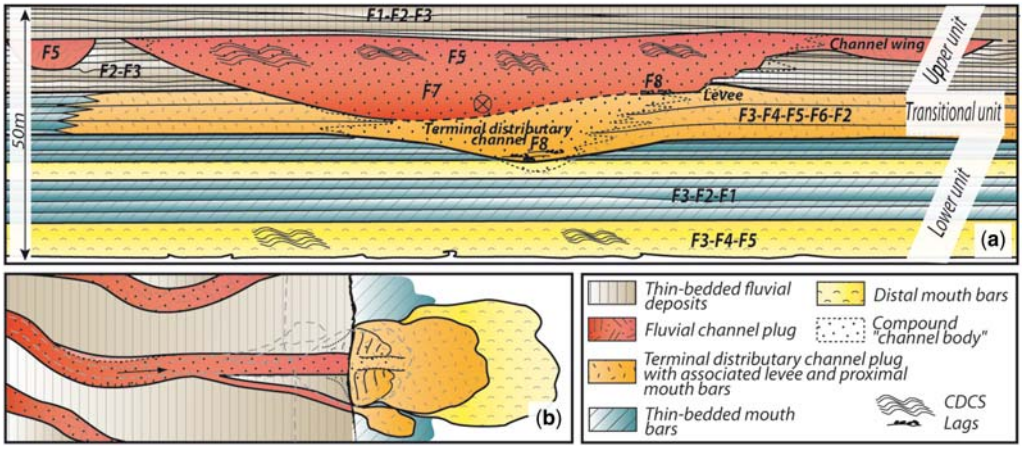

Fig. 9. Synthetic architectural (**a**) and depositional (**b**) models illustrating the location of channelized sandstone bodies at the top of a prograding mouth-bar system built from river jet effluxes. Facies codes are given in Table 1. Channelized sandstone bodies represent plugs of fluvioglacial channels passing downstream in subaqueous terminal distributary channels.

related to high-magnitude floods. Laterally, thinner-bedded mouth-bar successions reflect lateral deceleration of expanding flows and/or similar but minor flood events deposited under waning turbulent flows.

In the upper unit, well-stratified thin-bedded fluvial deposits are dominated by upper-stage plane beds, with occasional ripples, lags of small rip-up clast, basal gutter casts and load structures (F3 and F2), all features that have strong similarities with successions interpreted as deposited by ephemeral sheet-flood braided streams (Tunbridge 1981; Delucca & Eriksson 1989; Olsen 1989; Dam & Andreasen 1990; Brierley 1996; Neef *et al.* 1996). If the latter most commonly characterize arid environments, ablation-related floods in pro-glacial braidplain settings also result in ephemeral sheet flows (Gomez *et al.* 2000; Maizels 2002; Carrivick & Russell 2007). The channel bodies, both of the large- and small-scale types, are devoid of accretion surfaces and are interpreted as sandy channel plugs. Infilling facies typically comprise waning-flow sequences from base to top: a scour-related surface, an ubiquitous upper-flow regime condition in the lower part (F7) and lower-flow regime conditions but with high-concentration sand-sized suspended load in the upper part (F5). Ubiquitous CDCS in the upper part of channel plugs attests to their relationship with high-magnitude glacial floods (Ghienne *et al.* 2010). Channel plugs encompassing an axial scour infill and adjacent wings suggest a flood-related channel widening and subsequent net aggradation of the depositional surface after the outburst event. Finally, the whole depositional system is considered to be an outwash braidplain, which recorded two distinct and alternating depositional regimes: 'normal' sedimentation upon sandy braidplain driven by ablation-related floods and outburst events resulting in channel plugging. Both regimes are also recorded downstream in mouth-bar environments (see above). The lack of argilaceous deposits is inherent both to their poor

Fig. 8. Depositional facies from the Wadi Aramat area (Tihemboka High, western Libya): (**a**) pairs of vertical or U-shaped, *Arenicolites*-type burrows in thin-bedded mouth bars (F3, lower unit); (**b**) thin-bedded sandstone with prevailing F3 facies in the upper unit (inter-channel area); (**c**) crude ripple cross-stratification in proximal mouth bars (F4, transitional unit); (**d**) intraformational conglomerates in the basal part of terminal distributary channel (F8, transitional unit); (**e**) vertically aggrading, low-relief, symmetrical and undulating lamination (dotted lines), with episodic crestal jumps (arrows), interpreted as climbing stationary antidunes in proximal mouth bars (F6, transitional unit); (**f**) vertical sheet-dewatering structures in thin-bedded mouth bars (F3, lower unit); (**g**) horizontal to subhorizontal, thick laminations, representing large-scale undulating bedforms in lower part of channel plug (F7, upper unit); (**h**) two-dimensional, stoss-depositional to vertically aggrading CDCS, in the upper part of a large-scale channelized sandstone body (F5, upper unit); (**i**) general view of horizontal to subhorizontal laminations, representing large-scale undulating bedforms (F7, upper unit); (**j**) small-scale subhorizontal to concave-up laminations, interpreted as antidune deposits in proximal mouth-bar deposits (F3, transitional unit).

Downloaded from https://www.lyellcollection.org by INIST-CNRS on Jun 16, 2026

preservation potential in pre-vegetation braided systems (Davies & Gibling 2010) and to the Late Ordovician sand-dominated system (Ghienne *et al.* 2010). Poor development of cross-stratified facies indicates that the background sedimentary record was dominated by ephemeral ablation-related processes rather than by deposits typifying perennial sand-dominated rivers (e.g. Cant & Walker 1975, 1978; Miall 1996).

Regional-scale channel distribution

Channels in map view

Channel body distribution based on satellite images give an outstanding impression of the organization of the pro-glacial delta plain (Fig. 10). The area under examination consists of a 50 km wide, 250 km long stripe in the Tassili N'Ajjer across the Algeria/Libya boundary. It comprises more than 340 sinuous to straight sandstone ribbons, termed 'cordons' by Beuf *et al.* (1971), which most often correspond to up to 10 km long channel bodies similar to those studied in the upper unit of the Wadi Aramat exposures. The longer bodies can be continuously traced for up to 16 km. Both the large- and small-scale types are recognized (Fig. 11). Within the topset succession, the present-day erosional surface intersects strata almost randomly and the map therefore does not represent an actual distribution of time-equivalent channels. For example, only a few channels are mapped in the area where the present-day surface mostly intersects late- to post-glacial shallow-marine deposits. Alternatively, in other places, channels are over-represented relative to inter-channel areas owing to the outcropping mode with preferential preservation of channel bodies as inverted topographies. In addition, detection of channel bodies varies with type of satellite images. In the Tihemboka High area, for which a high-quality Spot image was available (spatial resolution of 2.5 m), a denser distribution of sandstone ribbons is found. Nevertheless, the channel body distribution faithfully reflects the pro-glacial palaeochannel networks and statistics can be performed.

Channel-body orientations have been analysed in two distinct areas with very similar patterns (Fig. 10), therefore allowing data to be mixed (Fig. 12a). Orientations of the channel bodies (longer than 0.5 km) range from 286°N to 28°N, with a mean at 294°N. Two thirds of the channel bodies are oriented towards the NNW (320–360°N). No variation is apparent when comparing proximal (southern) and distal (northern) contexts. However, in the western part of the mapped area (Fig. 10), a distinct set of wider channel bodies is seen, which we suspect belong to another glacial sequence. Channel bodies then appear basically parallel to each other, corresponding to linear drainage networks throughout the area. In addition, a number of channel bifurcations have been mapped. A succeeding confluence may arise at the kilometre scale, which mimics braidbar morphologies. Some of the large-scale channel bodies have neither confluence nor bifurcation along their entire exposed length. Channel bodies are straight, with sinuosity (length of channel thalweg/length of segment) less than 1.05 or faintly sinuous (1.1–1.5), although rare sinuous examples (1.2–1.35) are recognized (e.g. Fig. 11)

Channel body architecture

Channel body widths (340 samples) and thicknesses (available for 224 bodies) have been systematically estimated based on measurements of residual inverted topographies. Sandstone ribbons have basically consistent width and sharp boundaries. However, in rare places on high-resolution satellite images (Fig. 11), a more intricate organization is revealed. Indeed, large-scale channel bodies comprise a sinuous, narrow and uninterrupted main ribbon twisting between almond-shape to crescentic bodies occupying concave bends. In addition, scroll bars (lateral accretion) have been suspected but correspond only to subordinate features. Therefore, on low-resolution images or on degraded exposures where the internal architecture is not highlighted, measured widths of sandstone ribbons may correspond either to that of the narrow central ribbon or to that of a larger-scale ribbon amalgamating the narrow ribbon and adjacent bodies (inset of Fig. 11). Sandstone ribbon widths vary in the 40–630 m range, two-thirds of them being in the 60–160 m range (Fig. 12b). The width/frequency bar chart illustrates a roughly unimodal distribution with a peak at a channel width of 100 m and a median at *c.*125 m (Fig. 12b). Measured thicknesses (224 measurements) correspond to minimum values, as thalweg incision depths are unknown. The channel bodies are 3–30 m thick, in good agreement with field studies (see above and Beuf *et al.* 1971). The width/thickness frequency bar chart (Fig. 12d) indicates W/T ratios in the 5–42 range, half of the W/T being in the 10–17 range. A polymodal distribution might be proposed, but the significance of distinct groups (e.g. 10–14, 15–20 and 22–27) has not been elucidated.

Interpretation

To interpret Figure 10 is not straightforward. For instance, in the context of a progradation, and assuming an ice front more or less stabilized to the south (see the 'Geological setting' section), it is unclear whether the picture is representative of the

Downloaded from https://www.lyellcollection.org by INIST-CNRS on Jun 16, 2026

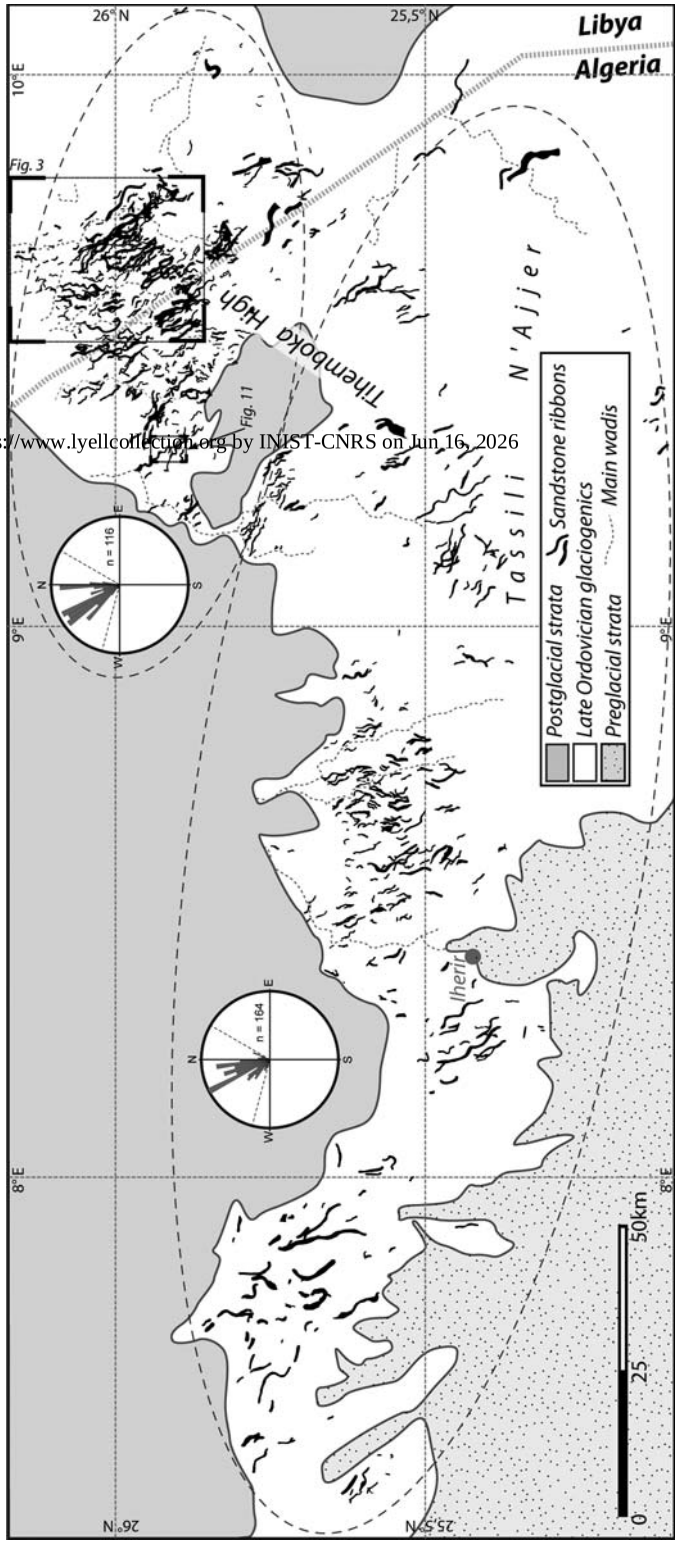

Fig. 10. Distribution of the channelized sandstone bodies ('cordons') throughout the Tassili N'Ajjer Plateau (modified from Beuf *et al.* 1971). Ranges of channel-body orientations of ribbons longer than 0.5 km are given for two distinct areas (envelope with dotted lines).

Downloaded from https://www.lyellcollection.org by INIST-CNRS on Jun 16, 2026

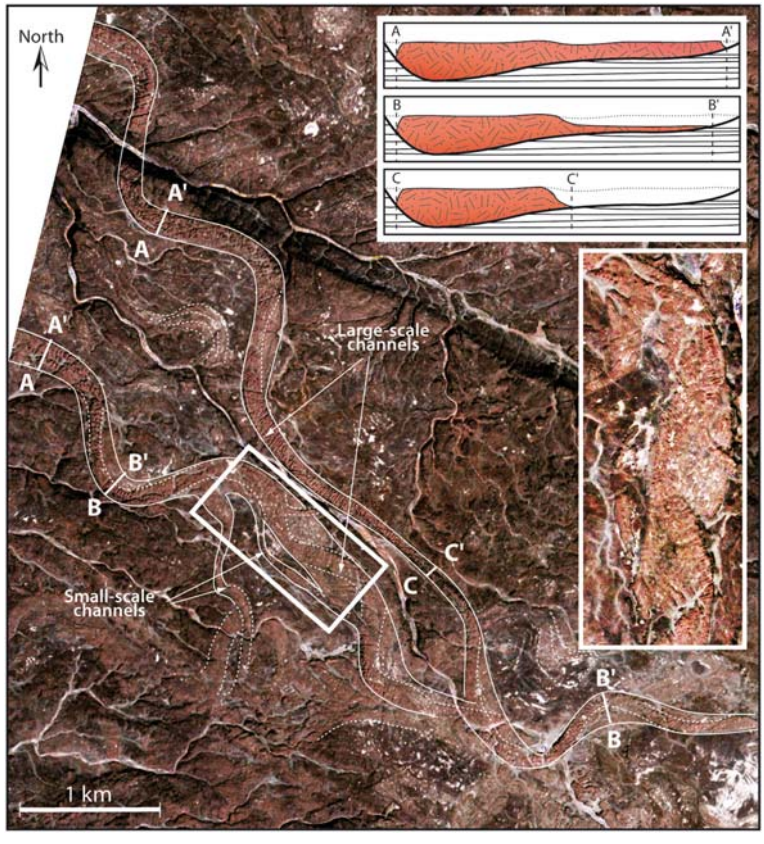

Fig. 11. Details of channelized sandstone bodies in the Algerian part of the Tihemboka High (Spot image), with a zoom (white rectangle) on a particular segment of an anastomosed sinuous channel. Internal geometries and different orders of channels are identifiable. The width of a sandstone ribbon depends on preservation: bankfull (A–A′), intermediate (B–B′) and low-stage (C–C′) cross-sections are seen.

entire 50 km long final channel networks extending from a pro-glacial zone to the south to river mouths to the north, or of the juxtaposition of diachronous final segments of a prograding river-mouth system progressively shifted basinward through time. Another limitation arises when considering channel branching patterns. The latter may represent either channel bifurcations within a distributary system (Olariu & Batthacharya 2006; North & Warwick 2007), bifurcations of braided channels (Rust 1978; Bristow & Best 1993; Ashworth *et al.* 2000) or channel avulsions and/or independent division and junction within an anastomosing network (Bristow 1996; Nanson & Knighton 1996; Makaske 2001; Twidale 2004). Channel-body bifurcations, however, do not represent a fundamental feature of the studied channel-body networks. More significant elements are (i) parallel channel bodies, with an averaged orientation that matches other regional-scale glacial and fluvial palaeoflow trends (Beuf *et al.* 1971; Ghienne *et al.* 2007*a*), (ii) almost constant width along an individual body and (iii) low sinuosities. Constant widths indicate that channel bodies generally do not include features related to lateral channel migration and constitute plug infills, in agreement with the interpretations based on outcrop sections. Scroll bars remain subordinate geometries, and true meandering system are absent (satellite image, cross-section), although they are recognizable in other glacial sequences (e.g. Rubino *et al.* 2003). This suggests that sinuous channel bodies from the Tassili N'Ajjer do not correspond to meandering channel plugs. However, geometries of large-scale channel bodies in detailed plane view attest in places that the differentiation of channels and of alternate bar-type sand-bodies can occur (Fig. 11). We suggest that they correspond to the plugs of respectively low-stage and bankfull channel cross-profiles, with variable preservation conditions (insets in Fig. 11). A former bar

Downloaded from https://www.lyellcollection.org by INIST-CNRS on Jun 16, 2026

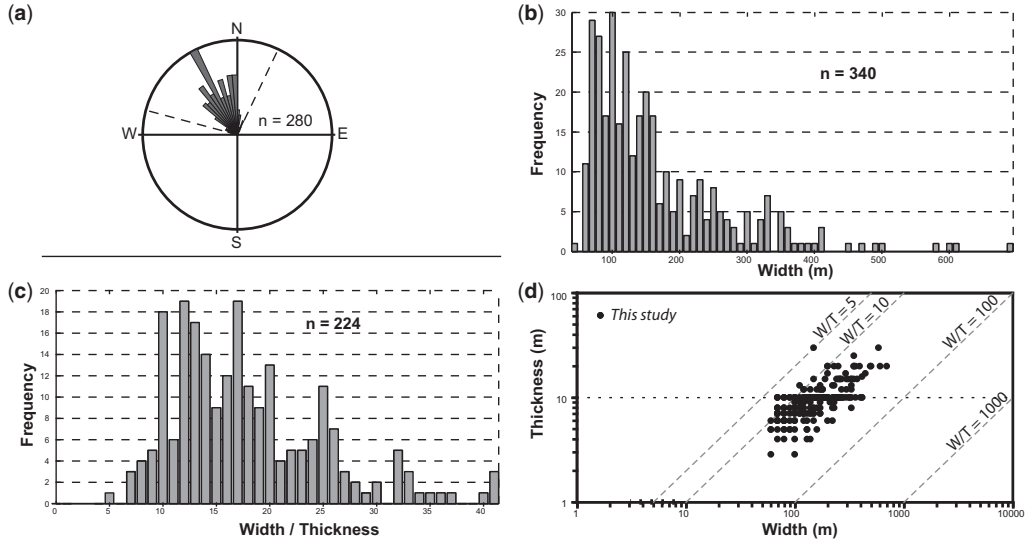

Fig. 12. Orientation trend (**a**) and widths (**b**) of channelized sandstone bodies (undifferentiated bankfull and low-stage cross-sections). (**c**) Frequency plot of the width (W) to thickness (T) ratio for ribbons mapped in Figure 10. (**d**) Width v. thickness plot for 224 ribbons, with a W/T mean value of 16.5.

geometry is inferred in underlying deposits, which should have existed before the channel plugging phase. Considering the size of the channel bodies (typically in the 60–600 m range; low-stage and bankfull sections undifferentiated) and genetic links between large- and small-scale bodies, they are thus best interpreted as plugs of braided channels with interlaced anastomosed sinuous channels.

Channels transferred meltwater and sediments from the ice-marginal zone to the river mouths, along a less than 50 km long pro-glacial plain. In a particular zone (e.g. the Tihemboka High, Fig. 10), no lateral differentiation or hierarchy is apparent, indicating a line source of sediment input points in front of the ice sheet. If trunk channels existed upstream, as suggested by the occurrence of deeply incised channels in relation to the pro-glacial zone (Ghienne *et al.* 2010), they should have been numerous and quite uniformly distributed through time and space (Russell *et al.* 2005). Nearby sediment input points did not allow individual fans to grow up, but instead favoured the development of many pro-glacial, adjacent and parallel elongated fans, the juxtaposition of which led to a virtually planar and unconfined outwash plain (Fig. 13). Such a uniform distributary network also implies a line source at river mouths, which characterizes a pro-glacial delta setting (Nemec & Steel 1988; Orton & Reading 1993). This is supported by the absence of clear distributary patterns within the preserved channel networks, even though some of them represent features close to the river mouth, as indicated by the stratigraphic architecture of the succession within which they are encased.

This proglacial outwash setting with moderate slope gradient (2 m km^{-1}) and migrating sediments input points (glacial outlets) may fundamentally differ from other better-known unconfined systems, such as higher-gradient aprons with a coarser sediment load and reduced water discharge, or low-gradient sand-dominated channel belts on megafans (Hartley *et al.* 2010). The best analogues are probably the coastal Icelandic sandur plains (Maizels 1997, 2002; Marren 2002, 2005), including interlaced anastomosed channels in addition to the features representative of the braidplain setting (Twidale 2004).

A last important point is to note that there is no significant difference in the orientation trend of channel bodies in the Tihemboka High and the more western area. Therefore, this tectonic element, although recurrently effective during the Lower Palaeozoic (Beuf *et al.* 1971), had no interference on the latest Ordovician depositional surface, indicating it was either inactive or with uplift rates largely less than outwash plain aggradation rates.

Discussion

Although unconfined braided fluvial systems featured pre-vegetation settings (e.g. Davies & Gibling 2010), pre- and post-glacial sandstone-dominated fluvial successions in Algeria and

Downloaded from https://www.lyellcollection.org by INIST-CNRS on Jun 16, 2026

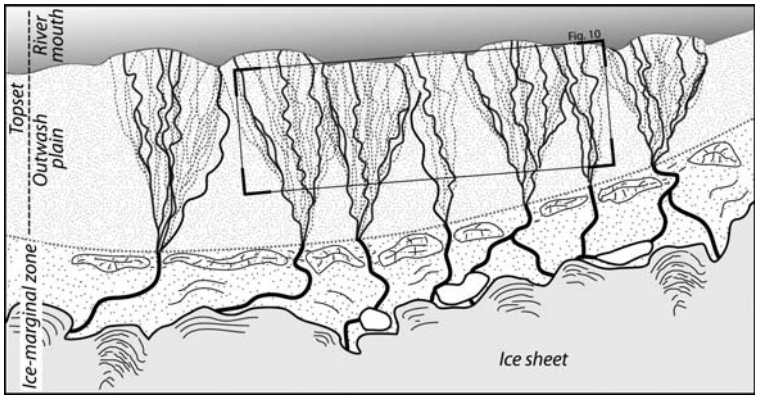

Fig. 13. Reconstructed map view of the studied Late Ordovician pro-glacial outwash braidplain that consists of unconfined fluvioglacial channel networks of adjacent elongated fans, including subordinate interlaced anastomosed sinuous channels. Sediment input points rapidly shifting through time and space in the ice-marginal zone result in a uniform distribution of the meltwater and sediment discharges upon the outwash plain and related braidplain deltas.

Libya (respectively Cambrian and Lower Devonian in age) lack any well-defined channel bodies cropping out in the form sandstone ribbons (Beuf *et al.* 1971; Eschard *et al.* 2005; Ghienne *et al.* 2007*b*). Instead, they are characterized by extensive cross-stratified sandstone sheets typically interpreted as braided stream deposits (e.g. Allen 1983; Gibling 2006). Hence, specific conditions may have arisen in the Late Ordovician paraglacial context that explain the profusion of ribbon-type channel bodies. We identified two potential dissimilarities that may have led to different paraglacial and non-glacial fluvial systems on the North Gondwana platform: (i) frozen outwash plains and (ii) the occurrence of high-magnitude outburst events. First, frozen sands enhancing bank stability (Syvitski 1986) can be suspected throughout the outwash plain. A consequence of this would have been the development of relatively deep channels, as suggested by the relatively low W/T ratios of the channel bodies. However, it is thought that frozen sands and bank stability should have resulted preferentially in meandering channel belts (cf. modern Siberian case studies, Sidorchuck *et al.* 2001) and such a model is rejected here. Instead, the outburst-related scheme is preferred because Late Ordovician sandstone ribbons are closely associated with the deposition of CDCS, which typify high-magnitude flood events related to glacier outbursts or jökulhlaups in sand-dominated systems (Ghienne *et al.* 2010).

In the case of braided channel belts, large- and small-scale channel bodies correspond to plugs of second- and third-order channels, respectively. Dealing with subordinate interlaced anastomosed channels, plugs relate either to low-stage or bankfull channel cross-sections. Distinct modes of channel plugging can have occurred separately or in combination through time and space. Indeed, plugs may have infilled abandoned channels, generating localized flow expansions and enhancing sand deposition from widespread, outwash-scale outburst-related sheet flows. Plugging stages may have also involved autocyclic processes alternating (during a flood peak) scour episodes with channel infilling stages, as investigated by Sheets *et al.* (2007) and Van Dijk *et al.* (2009). The plugging phase could alternatively occur during waning-stage flow conditions of outburst events, within an overall backstepping of the place of deposition from distal mouth-bar environments to the outwash channels (Hopkins 1985; Mulder *et al.* 1998; Olariu & Bhattacharya 2006; Van Dijk *et al.* 2009). Whatever the plugging mode or combination of modes, the plugs fossilized the channel networks, offering outburst-related snapshots of the outwash-braidplain organization. However, first-order channel belt boundaries are not identified, and it is unknown whether they correspond to either separate kilometre-scale wide features or contiguous channel belts forming a virtually continuous braidplain throughout the whole outwash surface. Inter-channel successions are interpreted as braid-bars and represent mostly the ablation-related background sedimentation that continuously aggraded over the whole outwash plain, interrupted by recurring outburst events. Flood-hardened or giant gravel bars that characterize outburst-dominated sandur plains (Marren 2005) are not present due to the absence of coarse material in the Late Ordovician glacial system.

Channel plugs are most probably diachronous across the Tassili N'Ajjer, considering that a single outburst resulting from the catastrophic drainage of subglacial meltwater storages should have only

Downloaded from https://www.lyellcollection.org by INIST-CNRS on Jun 16, 2026

affected a restricted, 10–50 km wide portion of the outwash plain (estimated maximum width is 50 km but it may be wider than this). Partial or complete plugging of the channels subsequent to an outburst event probably promoted avulsions and redistribution of the channels and/or the uncharacterized first-order channel belts across the outwash plain.

Plug-related channel bodies imply that the W/T ratios of channel bodies essentially reflect the W/T ratios of the formative channels. Except for channels only just scoured during the outburst event, we can expect a flood-related alteration of W/T ratios of pre-flood sinuous channels. In particular, widening and/or deepening of the pre-flood channel cross-section may occur during major flood events (Bristow 1996). As the channel bodies have thicknesses in the range 5–30 m, with a mean width of 120–130 m and a mean W/T of 16–17 (Fig. 12), they are included in the narrow ribbons to broad sheets categories according to

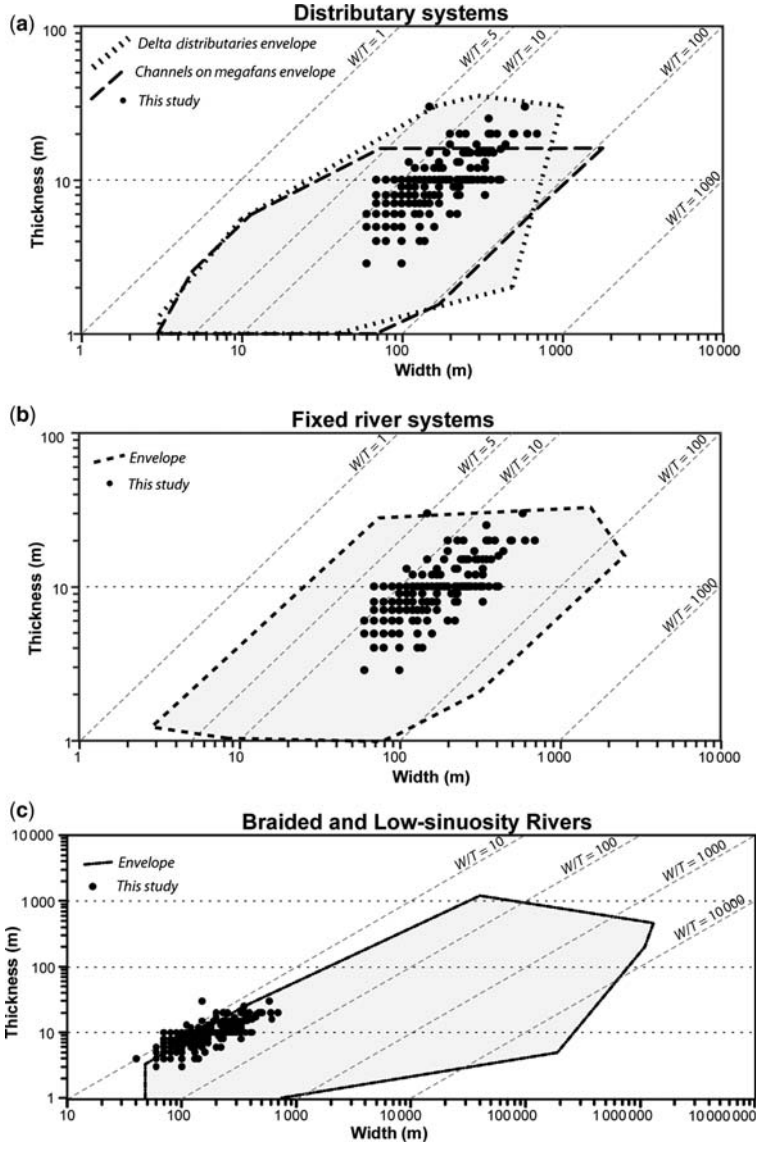

Fig. 14. Width v. thickness plots and associated envelopes for (**a**) distributary systems, (**b**) fixed river systems and (**c**) braided and low-sinuosity rivers (from Gibling 2006), compared with the data set of the present study.

Downloaded from https://www.lyellcollection.org by INIST-CNRS on Jun 16, 2026

the classification of Gibling (2006). The Late Ordovician data set has been plotted in W/T graphs (Figs 12d & 14) and is compared with the envelopes of three categories proposed by Gibling (2006): distributary systems, fixed river systems, and braided and low-sinuosity rivers (Fig. 14a–c). Our data set best fits the two former categories, although it has been related to a system analogous to the latter. Unsurprisingly, as the Late Ordovician channel bodies correspond to plugs, their W/T ratio does not fit the bodies representing long-lived evolutions including significant lateral migrations that usually characterize braided river systems. They probably resemble the fixed river and distributary systems because the latter are more frequently, on a geological timescale, affected by avulsion, a process that 'freezes' segments of the channel network, similar to the snapshots related to the outburst-related plug events over the Late Ordovician outwash plain.

Whatever the W/T ratio, the preserved channel bodies have similarities to both the active and abandoned pro-glacial drainage patterns of the modern marine Icelandic sandar often referred to as an unconfined braidplain. However, although the overall contexts are closely comparable in terms of geomorphology, short-term landscape development and hydraulic processes during outburst floods, important differences may be responsible for the distinct resulting stratigraphic architectures and sedimentary records. Indeed, wave-dominated shorelines in Iceland have not been recognized so far in the toe of the Late Ordovician outwash plains. Moreover, coarser sediments with prevailing bedload processes characterize the Icelandic outwash plains, in contrast to the significant suspended-load processes in the sand-dominated Late Ordovician counterpart (Ghienne *et al.* 2010). More detailed analogies between channel bodies in Late Ordovician and present-day distal segments of the pro-glacial outwash plains would require a deeper characterization of the stratigraphic record of the latter, especially at the scale of the entire aggradational–progradational wedge (seismic scale).

Conclusion

The large-scale stratigraphic architecture of pro-glacial outwash plains is intimately controlled by ice-front evolution, with for instance aggradation phases related to glacial advances. Sedimentation over the outwash plains also has a number of distinctions directly linked to the pro-glacial setting, which is responsible for the alternation of high-frequency/low-magnitude events with low-frequency/high-magnitude events, within systems dominated by high meltwater and sediment discharges. Numerous subglacial outlets, either penecontemporaneous or diachronous, but rapidly shifting through time within the ice-marginal zone, result in a distributary pattern that occurs essentially upstream of the outwash plain. Such an outwash plain comprises a succession of juxtaposed elongate fans, which forced each other together to flow basinward with limited possibilities for developing apparent lobate geometries. These processes resulted in a somewhat planar outwash plain and, downstream, braidplain-delta patterns. The occurrence of glacial outbursts in the Late Ordovician (which were able to plug the pre-flood channel networks), active as well as inactive channels, or new scours, offers snapshots of the outwash channel distribution in the form of an extensive array of sandstone ribbons that are presently exposed as inverted topographies in the Tassili N'Ajjer area.

The authors gratefully acknowledge TOTAL for financial, technical and scientific support and the National Oil Company of Libya for facilities during fieldwork. We are grateful to J. Melvin and an anonymous reviewer for their careful and constructive review of the manuscript.

References

Alexander, J., Bridge, J. S., Cheel, R. J. & Leclair, S. F. 2001. Bedforms and associated sedimentary structures formed under supercritical water flows over aggrading sand beds. *Sedimentology*, **48**, 133–152.

Allen, J. R. L. 1983. Studies in fluviatile sedimentation: bars, bar-complexes and sandstone sheets (low-sinuosity braided streams) in the brownstones (L. Devonian), Welsh Borders. *Sedimentary Geology*, **33**, 237–293.

Ashworth, P. J., Best, J. L., Roden, J. E., Bristow, C. S. & Klaassen, G. J. 2000. Morphological evolution and dynamics of a large, sand braid-bar, Jamuna River, Bangladesh. *Sedimentology*, **47**, 533–555.

Bellini, E. & Massa, D. 1980. A stratigraphic contribution to the Paleozoic of the Southern Basins of Libya. *In*: Salem, M. J. & Bursrevil, M. T. (eds) *The Geology of Libya*. Academic Press, London, **I**, 1–56.

Beuf, S., Biju-Duval, B., De Charpal, O., Rognon, P., Gariel, O. & Bennacef, A. 1971. *Les grès du Paléozoique inférieur au Sahara*. Science et Technique du Pétrole, **18**, Paris, 464.

Björnsson, H. 2002. Subglacial lakes in Iceland. *Global Planetary Change*, **35**, 255–271.

Boothroyd, J. C. & Nummedal, D. 1978. Proglacial braided outwash: a model for humid alluvial-fan deposits. *Canadian Society of Petroleum Geologists Memoir*, **5**, 641–668.

Brierley, G. J. 1996. Channel morphology and element assemblages: a constructivist approach to facies modelling. *In*: Carling, P. A. & Dawson, M. R. (eds) *Advances in Fluvial Dynamics and Stratigraphy*. West Sussex, England, John Wiley & Sons, 263–298.

Bristow, C. 1996. Reconstructing fluvial channel morphology from sedimentary sequences. *In*: Carling,

Downloaded from https://www.lyellcollection.org by INIST-CNRS on Jun 16, 2026

P. A. & Dawson, M. R. (eds) *Advances in Fluvial Dynamics and Stratigraphy*. West Sussex, England, John Wiley & Sons, 350–371.

Bristow, C. S. & Best, J. L. 1993. Braided rivers: perspectives and problems. *In*: Best, J. L. & Bristow, C. S. (eds) *Braided Rivers*. Geological Society, London, Special Publications, **75**, 1–11.

Buatois, L. A., Mangáno, M. G., Alissa, A. & Carr, T. R. 2002. Sequence stratigraphic and sedimentologic significance of biogenic structures from a Late Paleozoic marginal- to open-marine reservoir, Morrow Sandstone, subsurface of southwest Kansas, USA. *Sedimentary Geology*, **152**, 99–132.

Cant, D. J. & Walker, R. G. 1975. Development of a braided-fluvial facies model for the Devonian Battery Point Sandstone, Québec. *Canadian Journal of Earth Science*, **13**, 102–119.

Cant, D. J. & Walker, R. G. 1978. Fluvial processes and facies sequences in the sandy braided South Saskatchewan River, Canada. *Sedimentology*, **25**, 625–648.

Carrivick, J. L. & Russell, A. J. 2007. Glacifluvial landforms of deposition. *In*: Elias, S. A. (ed.) *Encyclopedia of Quaternary Science*. Elsevier, B.V., Amsterdam, **2**, 909–919.

Church, M. 1972. Baffin Island sandurs: a study of Arctic fluvial processes. *Geological Survey of Canada Bulletin*, **216**.

Coward, M. P. & Ries, A. C. 2003. Tectonic development of North African basins. *In*: Arthur, T. J. & MacGregor, D. S. (eds) *Petroleum Geology of Africa: New Themes and Developing Technologies*. Geological Society, London, Special Publications, **207**, 61–83.

Dam, G. & Andreasen, F. 1990. High-energy ephemeral stream deltas: an example from the upper Silurian Holmestrand Formation of the Oslo Region, Norway. *Sedimentary Geology*, **66**, 197–225.

Davies, N. S. & Gibling, M. R. 2010. Cambrian to Devonian evolution of alluvial systems: the sedimentological impact of the earliest land plants. *Earth-Science Reviews*, **98**, 171–200.

Dawson, M. R. & Bryant, I. D. 1987. Three-dimensional facies geometry in Pleistocene outwash sediments, Worcestershire, U.K. *The Society of Economic Paleontologists and Mineralogists*, **39**, 191–196.

Delucca, J. L. & Eriksson, K. A. 1989. Controls on synchronous ephemeral- and perennial-river sedimentation in the middle sandstone member of the Triassic Chinle Formation, northeastern New Mexico, U.S.A. *Sedimentary Geology*, **61**, 155–175.

Droser, M. L., Hugues, N. C. & Jell, P. A. 1994. Infaunal communities and tiering in Early Palaeozoic nearshore clastic environments: trace-fossil evidence from the Cambro-Ordovician of New South Wales. *Lethaia*, **27**, 273–283.

Duller, R. A., Mountney, N. P., Russell, A. J. & Cassidy, N. C. 2008. Architectural analysis of a volcaniclastic jökulhlaup deposit, southern Iceland: sedimentary evidence for supercritical flow. *Sedimentology*, **55**, 939–964.

Edmonds, D. A. & Slingerland, R. L. 2007. Mechanics of river mouth bar formation: implications for the morphodynamics of delta distributary networks. *Journal of Geophysical Research*, **112**, F02034, DOI:10.1029/2006JF000574.

Eschard, R., Abdallah, H., Braik, F. & Desaubliaux, G. 2005. The Lower Paleozoic succession in the Tasilli outcrops, Algeria: sedimentology and sequence stratigraphy. *First Break*, **23**, 27–36.

Fabre, J. & Kazi-Tani, N. 2005. Ordovicien, Silurien, Devonien, Permo-Carbonifère. *In*: Fabre, J. (ed.) *Géologie du Sahara occidental et central*. Tervuren African Geoscience Collection 108. Musée Royal de l'Afrique Centrale, Tervuren, 147–360.

Fielding, C. R. 2006. Upper flow regime sheets, lenses and scour fills: extending the range of architectural elements for fluvial sediment bodies. *Sedimentary Geology*, **190**, 227–240.

Fielding, C. R., Trueman, J. D. & Alexander, J. 2005. Sharp-based, flood-dominated mouth bars sands from the Burdekin River Delta of northeastern Australia: extending the spectrum of mouth-bar facies, geometry, and stacking patterns. *Journal of Sedimentary Research*, **75**, 55–66.

Friend, P. F. 1983. Towards the field classification of alluvial architecture or sequence. *In*: Collinson, J. D. & Lewin, J. (eds) *Modern and Ancient Fluvial Systems.* International Association of Sedimentologists, Boston, Special Publication, **6**, 345–354.

Galeazzi, S., Point, O., Haddadi, N., Mather, J. & Druesne, D. 2010. Regional geology and petroleum systems of the Illizi–Berkine area of the Algerian Saharan Platform: an overview. *Marine and Petroleum Geology*, **27**, 143–178.

Gerard, J. R. F. & Bromley, R. G. 2008. *Ichnofabrics in Clastic Sediments: Application to Sedimentological Core Study, a Practical Guide*. J. Gerard, Madrid.

Ghienne, J.-F. 2003. Late Ordovician sedimentary environments, glacial cycles, and post-glacial transgression in the Taoudeni Basin, West Africa. *Palaeogeography, Palaeoclimatology, Palaeoecology*, **189**, 117–145.

Ghienne, J.-F., Boumendjel, K., Paris, F., Videt, B., Racheboeuf, P. & Ait Salem, H. 2007*a*. The Cambrian–Ordovician succession in the Ougarta Range (western Algeria, North Africa) and interference of the Late Ordovician glaciation on the development of the Lower Palaeozoic transgression on northern Gondwana. *Bulletin of Geosciences*, **82**, 183–214.

Ghienne, J.-F., Le Heron, D., Moreau, J., Denis, M. & Deynoux, M. 2007*b*. The Late Ordovician glacial sedimentary system of the North Gondwana platform. *In*: Hambrey, M., Christoffersen, P., Glasser, N., Janssen, P., Hubbard, B. & Siegert, M. (eds) *Glacial Sedimentary Processes and Products*. Internal Association of Sedimentologists, Oxford, Special Publication, **39**, 295–319.

Ghienne, J.-F., Girard, F., Moreau, J. & Rubino, J.-L. 2010. Late Ordovician climbing-dune cross-stratification: a signature of outburst bloods in proglacial outwash environments? *Sedimentology*, **57**, 1175–1198, DOI: 10.1111/j.1365-3091.2009.01142.x.

Gibling, M. R. 2006. Width and thickness of fluvial channel bodies and valley fills in the geological record: a literature compilation and classification. *Journal of Sedimentary Research*, **76**, 731–770.

Downloaded from https://www.lyellcollection.org by INIST-CNRS on Jun 16, 2026

GOMEZ, B., SMITH, L. C., MAGILLIGAN, F. J., MERTES, L. A. K. & SMITH, N. D. 2000. Glacier outburst floods and outwash plain development: Skeidarársandur, Iceland. *Terra Nova*, **12**, 126–131.

HARTLEY, A. J., WEISSMAN, G. S., NICHOLS, G. J. & WARWICK, G. L. 2010. Large distributive fluvial systems: characteristics, distribution, and controls on development. *Journal of Sedimentary Research*, **80**, 167–183.

HIRST, J. P. P., BENBAKIR, A., PAYNE, D. F. & WESTLAKE, I. R. 2002. Tunnel valleys and density flow processes in the upper Ordovician glacial succession, Illizi Basin, Algeria: influence on reservoir quality. *Marine Petroleum Geology*, **25**, 297–324.

HOPKINS, J. C. 1985. Channel-fill deposits formed by aggradation in deeply scoured, superimposed distributaries of the Lower Kootenai Formation (Cretaceous). *Journal of Sedimentary Petrology*, **55**, 42–52.

HOYAL, D. C. J. D., VAN WAGONER, J. C. *ET AL.* 2003. Sedimentation from jets: a depositional model for clastic deposits of all scales and environments. *American Association of Petroleum Geologists*, Search and Discovery, Online article #40082.

KRZYSZKOWSKI, D. 2002. Sedimentary successions in ice-marginal fans of the Late Saalian glaciation, southwestern Poland. *Sedimentary Geology*, **149**, 93–109.

LANGFORD, R. & BRACKEN, B. 1987. Medano Creek, Colorado, a model for upper-flow-regime fluvial deposition. *Journal of Sedimentary Petrology*, **57**, 863–870.

LE HERON, D. P. & CRAIG, J. 2008. First order reconstructions of a Late Ordovician Saharan ice sheet. *Journal of the Geological Society, London*, **165**, 19–29.

LE HERON, D. P., CRAIG, J., SUTCLIFFE, O. & WHITTINGTON, R. 2006. Late Ordovician glaciogenic reservoir heterogeneity: an example from the Murzuq Basin, Libya. *Marine and Petroleum Geology*, **23**, 655–677.

LE HERON, D., CRAIG, J. & ETIENNE, J. L. 2009. Ancient glaciations and hydrocarbon accumulations in North Africa and the Middle East. *Earth-Science Reviews*, **93**, 47–76.

LOI, A., GHIENNE, J.-F. *ET AL.* 2010. The Late Ordovician glacio-eustatic record from a high-latitude storm-dominated shelf succession: the Bou Ingarf section (Anti-Atlas, Southern Morocco). *Palaeogeography, Palaeoclimatology, Palaeoecology*, **296**, 332–358, DOI: 10.1016/j.palaeo.2010.01.018.

LOWE, D. R. 1975. Water escape structures in coarse-grained sediments. *Sedimentology*, **22**, 157–204.

MAGILLIGAN, F. J., GOMEZ, B., MERTES, L. A. K., SMITH, L. C., SMITH, N. D., FINNEGAN, D. & GARVIN, J. B. 2002. Geomorphic effectiveness, sandur development, and the pattern of landscape response during jökulhlaups: Skeidarársandur, southeastern Iceland. *Geomorphology*, **44**, 95–113.

MAIZELS, J. K. 1993. Lithofacies variations within sandur deposits: the role of runoff regime, flow dynamics and sediment supply characteristics. *Sedimentary Geology*, **85**, 299–325.

MAIZELS, J. K. 1997. Jökulhlaup deposits in proglacial areas. *Quaternary Science Reviews*, **16**, 793–819.

MAIZELS, J. 2002. Sediments and landforms of modern proglacial terrestrial environments. *In*: MENZIES, J. (ed.) *Modern and Past Glacial Environments*. Butterworth-Heinemann, Oxford, 279–316.

MAKASKE, B. 2001. Anastomosing rivers: a review of their classification, origin and sedimentary products. *Earth-Science Reviews*, **53**, 149–196.

MARREN, P. M. 2002. Fluvial–lacustrine interaction on Skeidarársandur, Iceland: implications for sandur evolution. *Sedimentary Geology*, **149**, 43–58.

MARREN, P. M. 2004. Present-day sandurs are not representative of the geological record. *Sedimentary Geology*, **164**, 335–340.

MARREN, P. M. 2005. Magnitude and frequency in proglacial rivers: a geomorphological and sedimentological perspective. *Earth-Science Reviews*, **70**, 203–251.

MELLERE, D., PLINK-BJÖRKLUND, P. & STEEL, R. J. 2002. Anatomy of shelf deltas at the edge of a prograding Eocene shelf margin, Spitsbergen. *Sedimentology*, **49**, 1181–1206.

MIALL, A. D. 1996. *The Geology of Fluvial Deposits*. New York, Springer-Verlag.

MOREAU, J., GHIENNE, J.-F., LE HERON, D., RUBINO, J.-L. & DEYNOUX, M. 2005. A 440 Ma old ice stream in North Africa. *Geology*, **33**, 753–756.

MULDER, T., SYVITSKI, J. P. M. & SKENE, K. I. 1998. Modelling of erosion and deposition by turbidity currents generated at river mouths. *Journal of Sedimentary Research*, **68**, 124–137.

MUTTI, E., TINTERI, R., BENEVELLI, G., DI BIASE, D. & CAVANNA, G. 2003. Deltaic, mixed and turbidite sedimentation of ancient foreland basins. *Marine and Petroleum Geology*, **20**, 733–755.

NANSON, G. C. & KNIGHTON, A. D. 1996. Anabranching rivers: their cause, character and classification. *Earth Surface Processes and Landforms*, **21**, 217–239.

NEEF, G., BOTRILL, R. S. & COHEN, D. R. 1996. Mid and Late Devonian arenites deposited by sheet-flood, braided streams and rivers in the northern Barrier Ranges, far western New South Wales, Australia. *Sedimentary Geology*, **103**, 39–61.

NEMEC, W. & STEEL, R. J. 1988. What is a fan delta and how do we recognize it? *In*: NEMEC, W. & STEEL, R. J. (eds) *Fan Deltas: Sedimentology and Tectonic Settings*. Blackie and Son, London, 3–22.

NORTH, C. P. & WARWICK, G. L. 2007. Fluvial fans: myths, misconceptions, and the end of the terminal-fan model. *Journal of Sedimentary Research*, **77**, 693–701.

OLARIU, C. & BHATTACHARYA, J. P. 2006. Terminal distributary channels and delta front architecture of river-dominated delta systems. *Journal of Sedimentary Research*, **76**, 212–233.

OLSEN, H. 1989. Sandstone-body structures and ephemeral stream processes in the Dinosaur Canyon Member, Moenave Formation (Lower Jurassic), Utah, U.S.A. *Sedimentary Geology*, **61**, 207–221.

ORTON, G. J. & READING, H. G. 1993. Variability of deltaic processes in terms of sediment supply, with particular emphasis on grain size. *Sedimentology*, **40**, 475–512.

PETERS, L. E., ANANDAKRISNAN, S., ALLEY, R. B. & SMITH, A. M. 2007. Extensive storage of basal meltwater in the onset region of a major West Antarctic ice stream. *Geology*, **35**, 251–254.

PLINK-BJÖRKLUND, P., MELLERE, D. & STEEL, R. J. 2001. Turbidite variability and architecture of sand-prone, deep-water slopes: Eocene clinoforms in the central

Downloaded from https://www.lyellcollection.org by INIST-CNRS on Jun 16, 2026

basin, Spitsbergen. *Journal of Sedimentary Research*, **71**, 895–912.

Rubino, J.-L., Anfray, R., Blanpied, C., Ghienne, J.-F. & Manatschal, G. 2003. Meander belt complex within the lower Mamuniyat Formation in western Al Qarqaf area, Libya. *In*: Salem, M. J. & Oun Khaled, M. (eds) *The Geology of Northwest Libya; Volume II, Sedimentary basins of Libya, Second Symposium*. Symposium on the Sedimentary Basins of Libya, **2**, 3–18.

Russell, A. J., Fay, H., Marren, P. M., Tweed, F. S. & Knudsen, Ó. 2005. Icelandic jökulhlaup impacts. *In*: Caseldine, C., Russell, A., Hardardottir, J. & Knudsen, Ó . (eds) *Iceland – Modern Processes and Past Environments*. Elsevier, Amsterdam-Boston-Heidelberg-London, Development in Quaternary Science, **5**, 153–203.

Russell, A. J. 2009. Jökulhlaup (ice-dammed lake outburst flood) impact within a valley-confined sandur subject to backwater conditions, Kangerlussuaq, West Greenland. *Sedimentary Geology*, **215**, 33–49.

Rust, B. R. 1978. A classification of alluvial channel systems. *In*: Miall, A. D. (ed.) *Fluvial Sedimentology*. Canadian Society of Petroleum Geologists Memoir, Calgary, **5**, 187–198.

Schomacker, E. R., Kjemperud, A. V., Nystuen, J. P. & Jarhen, J. S. 2010. Recognition and significance of sharp-based mouth-bar deposits in the Eocene Green River Formation, Uinta Basin, Utah. *Sedimentology*, **57**, 1069–1087.

Sheets, B. A., Paola, C. & Kelberer, J. M. 2007. Creation and preservation of channel-form sand bodies in an experimental alluvial system. *In*: Nichols, G. J., Williams, E. & Paola, C. (eds) *Sedimentary Processes, Environments and Basins – a tribute to Peter Friend*. International Association of Sedimentologists, Blackwell, Oxford, Special Publication, **38**, 555–567.

Sidorchuk, A., Borisova, O. & Panin, A. 2001. Fluvial response to the Late Valdai/Holocene environmental change on the East European Plain. *Global and Planetary Change*, **28**, 303–318.

Smith, L. C., Sheng, Y. *et al.* 2006. Geomorphic impact and rapid subsequent recovery from the 1996 Skeidarársandur jökulhlaup, Iceland, measured with multi-year airbone lidar. *Geomorphology*, **75**, 65–75.

Snorrason, Á., Jónsson, P., Sigurdsson, O., Pálsson, S., Árnasson, S., Vikingsson, S. & Kaldal, I. 2002. November 1996 jökulhlaup on Skeidarársandur outwash plain, Iceland. *In*: Martini, I. P., Baker, V. R. & Garzón, G. (eds) *Flood and Megaflood Processes and Deposits: Recent and Ancient Examples*. International Association of Sedimentologists, Oxford, Special Publication, **32**, 55–65.

Spinewine, B., Sequeiros, O. E., Garcia, M. H., Beaubouef, R. T., Sun, T., Savoye, B. & Parker, G. 2009. Experiments on wedge-shaped deep-sea sedimentary deposits in minibasins and/or on channel levees emplaced by turbidity currents. Part II: Morphodynamic evolution of the wedge and of the associated bedforms. *Journal of Sedimentary Research*, **79**, 608–628.

Sutter, J. R. 1994. Deltaic coasts. *In*: Carter, R. W. G. & Woodroffe, C. D. (eds) *Coastal Evolution: Late Quaternary Shoreline Morphodynamics*. Cambridge University Press, Cambridge, 87–120.

Syvitski, J. P. M. 1986. Estuaries, deltas and fjords of eastern Canada. *Geoscience Canada*, **13**, 91–100.

Tunbridge, I. P. 1981. Sandy high-energy flood sedimentation – some criteria for recognition, with an example from the Devonian of S.W. England. *Sedimentary Geology*, **28**, 79–95.

Twidale, C. R. 2004. River patterns and their meaning. *Earth-Science Reviews*, **67**, 159–218.

Van Dijk, M., Postma, G. & Kleinhans, M. G. 2009. Autocyclic behaviour of fan deltas: an analogue experimental study. *Sedimentology*, **56**, 1569–1589.

Winsemann, J., Hornung, J. J. *et al.* 2009. Anatomy of a subaqueous ice–contact fan and delta complex, Middle Pleistocene, North-west Germany. *Sedimentology*, **56**, 1041–1076.

Zielinski, T. & Van Loon, A. J. 2002. Present-day sandurs are not representative of the geological record. *Sedimentary Geology*, **152**, 1–5.

Zielinski, T. & Van Loon, A. J. 2003. Pleistocene sandur deposits represent braidplains, not alluvial fans. *Boreas*, **32**, 590–611.